Continental Shelf Research
November 2022, Volume 250 Pages 104843 (17p.)
https://doi.org/10.1016/j.csr.2022.104843
https://archimer.ifremer.fr/doc/00919/103065/

Sporadic wind-driven upwelling/downwelling and associated cooling/warming along Northwestern Mediterranean coastlines

Odic Roxane [1], Bensoussan Nathaniel [1], Pinazo Christel [1], Taupier-Letage Isabelle [1], Rossi Vincent [1, *]

[1] Aix Marseille Université, Université de Toulon, CNRS, IRD, MIO UM 110 UMR 7294, 13288, Marseille, France

* Corresponding author : Vincent Rossi, email address : vincent.rossi@mio.osupytheas.fr

Abstract :

Intermittent wind-driven coastal upwelling and downwelling are ubiquitous processes that drive a large part of the high frequency variability of coastal hydrography, with potential implications for ecosystems and socio-economic activities. Little synoptic information exists however on these processes, especially in regions characterized by rapidly changing atmospheric forcing and complex shorelines. Combining multi-annual hourly observations of nearshore temperatures with a long-term archive of Sea Surface Winds (SSW from ERA5 reanalysis), we investigate the statistical occurrence of wind-driven upwelling and downwelling events and their associated thermal responses along the northwestern Mediterranean coastlines. A Wind-based Upwelling and Downwelling Index (WUDI) is calculated at 20 km spatial resolution and validated against time-series of surface and subsurface in-situ temperatures at 11 coastal locations.

We find that the WUDI index allows monitoring robustly all year round both up-and downwelling intermittent events that effectively cause coastal cooling/warming. On average, significant thermal responses to favorable winds appear after short delays (spanning 6-54 h for upwelling, 12-66 h for downwelling, depending on the site considered) with intensities 5 to 10 times stronger in stratified as compared to non-stratified conditions. Maximum near-surface cooling (subsurface warming, respectively) recorded after the most extreme events can reach up to-12.5 degrees C (+11 degrees C, respectively) during the period of seasonal stratification.

A climatological database of wind-driven events that can be associated with typical thermal responses is constructed for the Northwestern Mediterranean shorelines over the last four decades. It shows that up/downwelling events are favored along certain portions of coastline, called "cells", and are characterized by specific magnitudes, frequencies of occurrence and durations with respect to seasonality. We demonstrate that shorelines ranging from 4.0 degrees E to 6.2 degrees E are dominated by wind-driven upwelling, while shorelines spanning 3.0-3.5 degrees E are dominated by wind-driven downwelling. Furthermore, it reveals previously overlooked cells, such as around Frejus/Cannes and Livorno/Piombino for upwelling and near Albengua for downwelling, which are however activated about 2-3 times less frequently than the prominent cells in the Gulf of Lion.

Despite differential responses, these wind-driven events are more frequent during winter-spring than during summer-autumn: for both upwelling and downwelling, the mean occurrences at the most active cells are 11 days per month in winter-spring compared to 8 days per month in summer-autumn. While the main upwelling (resp. downwelling) events are generated by the prevailing northwesterlies (resp. easterlies), both winds also force the opposite process depending on the shoreline orientation and small changes in wind direction.

Graphical abstract

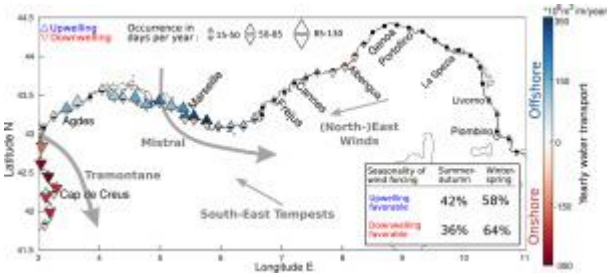

Highlights

► Wind-based Upwelling–Downwelling Index (WUDI) to study sporadic coastal processes. ► Statistical analyses of WUDI and temperature time-series at each 20-km coastal cell. ► Up/downwelling-favorable winds cause slightly delayed and transient cooling/warming. ► Thermal responses are 5–10 times stronger in stratified vs non-stratified periods. ► Up/downwelling events occur at some cells with specific frequency and strength.

Keywords : Sporadic upwelling, downwelling, Events analysis, Northwestern Mediterranean Sea, Wind-based Upwelling and Downwelling Index, Coastal cooling, warming, Sea Surface Wind, ERA5 Reanalysis

1. Introduction

Coastal upwelling and downwelling processes are ubiquitous phenomena involving horizontal and vertical movements of water masses near the coast, the main driver being the winds blowing on the surface ocean (Bakun 1973). An upwelling event is generally signed by decreasing Sea Surface Temperature (SST) associated with a relative increase of nutrients, while a downwelling event causes coastal warming and nutrient depletion. This is because, in the commonly stratified ocean, subsurface waters tend to be colder and richer in nutrients than the warm and nutrient-depleted upper layers. Hence, downwelling and upwelling processes have been shown to impact both water column hydrography and surface nutrient concentrations of the coastal ocean, having important consequences for plankton productivity and community composition (Chavez and Messié 2009; Rossi et al. 2013; García-Reyes et al. 2014; Armbrecht et al. 2014).

These physical processes are forced by persistent or sporadic alongshore winds (i.e., parallel to the main orientation of the coast). The direction of the Sea Surface Winds (SSW) determines the coastal horizontal divergence/convergence, itself controlling the upward/downward vertical water movement. At first order, the intensity, periodicity and timing of the wind forcing control the intermittence of these phenomena and the magnitude of their impacts (Rossi et al. 2014).

The world's most intense wind-driven coastal upwelling areas, usually referred to as the Eastern Boundary Upwelling Systems (EBUS), are zones where, due to the action of the trade winds generated by quasi-stationary high-pressure cells, cold and nutrient-rich subsurface waters are upwelled to the surface almost all year long (Rossi et al. 2009). The primary mechanism for those large-scale upwelling systems is the offshore Ekman transport, induced by quasi-permanent alongshore wind stress. Moreover, many recent studies demonstrated the existence of intermittent downwelling/upwelling cells of restricted spatial extensions, situated in coastal loca-

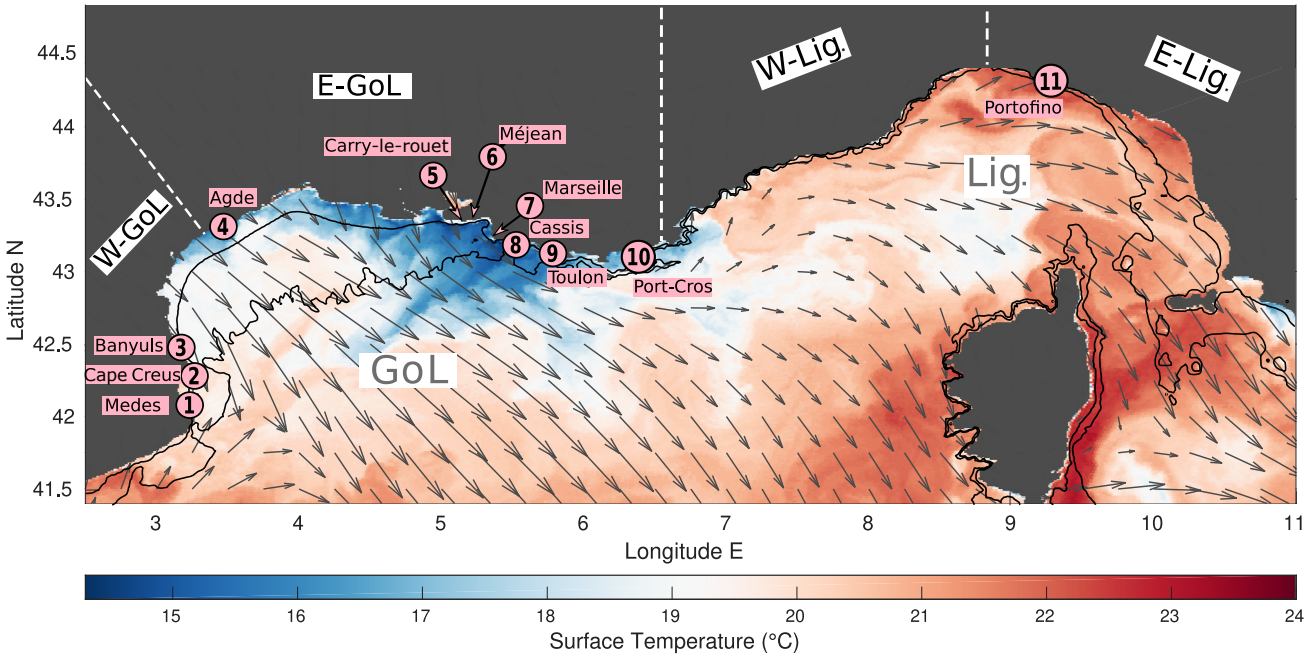

Figure 1: Exemplary upwelling event forced by northwestern winds (grey arrows, instantaneous 10-m SSW from ERA5 Reanalysis on 15/07/2012 at 18h) that caused persistent surface cooling (skin Sea Surface Temperature derived from AVHRR satellite imagery on 18/07/2012 extracted from the OSIS database (Taupier-Letage 2008) along the North-West Mediterranean coastlines. The 11 coastal locations where *in-situ* temperatures were monitored (part of the T-MEDNet monitoring network) are indicated as pink circles. The black iso-curves represent the 50 m and 200 m isobaths. The coastline is divided in 4 parts (delimited by the white dotted lines) with respect to its general orientation, namely W-GoL, E-GoL (Western/Eastern Gulf of Lion) and W-Lig, E-Lig (Western/Eastern Liguria).

tions that do not belong to the EBUS. These sporadic wind-driven processes are forced by highly variable local wind patterns, alternating between favorable and unfavorable forcing. Coastal regions of the worldwide ocean that are subjected to such sporadic wind-driven processes include, for example, the South-East Australian shores (Rossi et al. 2014), the South Brazilian Bight (Palma and Matano 2009), the Yucatan peninsula (Reyes-Mendoza et al. 2016), and some locations of the Mediterranean Sea (Johns et al. 1992; Millot 1979; Bakun and Agostini 2001). Despite the different climatic and oceanic contexts, all these coastal regions are characterized by the repeated occurrence of short-living but significant warming/cooling events forced by local winds.

In the northwestern Mediterranean, the prevailing Mistral wind is known as upwelling favorable (Millot 1979). This intense northerly wind is generated by a synoptic air current that accelerates after penetrating the Rhône corridor (Jacox et al. 2014; Obermann-Hellhund et al. 2018), often occurring simultaneously with the Tramontane wind. When both reach the sea they tend to veer so that they are described as strong northwesterly winds, most often associated with clear sky. In summer, they episodically blow for periods of few days with mean speeds of 10-15 m.s^{-1} and they are stronger (up to 25 m.s^{-1}) and last longer in winter (Millot 1990; Jacq et al. 2005). According to Jacq et al. (2005) a Mistral event of more than 10 consecutive days is rare and the longest event recorded in-land lasted 16 days. Although less frequent than the northwesterly, the period of autumn to spring is also known to yield violent southeasterly winds that can occasionally reach speed up to 25 m.s^{-1} in the North-Western Mediterranean basin (Millot 1990).

The current understanding of coastal up/downwellings in the North-West Mediterranean Sea relies on few numerical modelling studies (Johns et al. 1992; André et al. 2005; Barrier et al. 2016), spatially-confined field studies (Pinazo et al. 2018) and regional (Millot 1990; Berta et al. 2018) to basin-scale perspectives (Bakun and Agostini 2001).

Millot (1979) used SST satellite imagery and *in-situ* temperature and current observations to demonstrate the existence of upwelling events along the French coastlines of the Gulf of Lion (GoL), related to strong Mistral events during summer. According to his results, upwelling can appear one or two days after intense Mistral winds of about 10 m.s^{-1} with an associated SST decrease of about -5°C in summer (Millot 1979). Field analysis of the 2012/2013 upwelling events occurring along the French Mediterranean coastlines in September-October showed a SST cooling of -5 to -6°C and lasted between 7 and 20 days, with a mean of 10 days (Pinazo et al. 2018). These events occur in spatially-restricted -or source points- upwelling cells with extensions ranging from 10 to 20 km of coastline (Millot and Wald 1981). Millot (1979) identified 6 upwelling cells named after the nearby cities: from West to East, Valras and Sète along the Languedoc coast, Les-Saintes-Maries and Faraman (Camargue) and finally the cells of Méjean (Côte Bleue) and Cassis (Calanques), which is the strongest one. Note that

Millot (1979) also documented a downwelling signal after a strong Mistral episode in the southwestern GoL but without characterizing further the event.

Using a climatological database of *in-situ* winds, Bakun and Agostini (2001) established an annual seasonality of upwelling and downwelling in the Mediterranean Sea. They found strong upwelling zones in the GoL, from Montpellier to Toulon, linked with the Mistral and Tramontane. They suggested that the GoL upwellings also occur in winter since it was when they estimated maximum intensity of wind-forced vertical movement of coastal waters. Bakun and Agostini (2001) also identified the Southwestern part of the GoL as subject to downwelling favorable wind forcing, particularly intense during winter.

Note that, as already documented elsewhere Oke and Middleton (2000), intense barotropic currents flowing northeastward (e.g. linked to particularly vigorous anticyclonic mesoscale eddies opposing the main westward flow associated with the Northern Current) encroaching onto the continental shelf (such as the one bordering the western GoL) could drive topographic or current-driven upwelling in the bottom boundary layer (i.e. whose thermal response is hardly detectable as being ephemeral, of low magnitude and confined to the subsurface). Other physical processes inducing slight upwelling and/or redistributing upwelled waters consist of spatially varying cross-shore currents, for instance due to the rare shelf-intrusions of the meandering northern current (Barrier et al. 2016) and/or to wind-driven currents interacting with angular coastlines (Crepon and Richez 1982; Crepon et al. 1984; Schaeffer et al. 2011). These processes are particularly relevant for the western GoL but are not studied here as the wind is neither the primary forcing mechanism nor inducing vertical movements.

Previous studies showed the existence of wind-driven processes and documented significant oceanic responses in the GoL but some coastlines were not systematically surveyed and their temporal variabilities remain unclear, especially the seasonality. The results of Millot (1979) were based on moorings (temperature, current), hydrological casts collected at a few locations and earlier SST images during several years but for limited durations. Conversely, the SSW dataset used by Bakun and Agostini (2001) had large spatial coverage but poor spatio-temporal resolutions that prevented a precise description of these small-scale and short-living processes. Moreover, while upwelling cells were identified by Millot (1979), it was not the case for the downwelling process (which is more difficult to evidence). The magnitude and temporal delay of the oceanic temperature response to favorable wind forcing were hardly quantified and just from a limited number of observations. For both upwelling and downwelling, the link between atmospheric forcing and ocean temperature has yet to be thoroughly described in our study area. To bridge this knowledge gap, we conduct here a statistical analysis of both up/downwelling events spanning a long time horizon along the North-West Mediterranean coastlines.

To conduct such study, one could exploit continuous remotely-sensed observations of both SSW and SST over the coastal zone; however, these gridded datasets offer limited capabilities because (i) coastal wind profiles remain poorly resolved by current satellite missions (Bourassa et al. 2019) and (ii) SST imagery contain gaps (clouds) or spurious flags, especially for the cold values indicative of upwelling (Taupier-Letage 2014; Meneghesso et al. 2020). Consequently, it may induce a spurious time-lag of several days for the detection of upwelling events as well as a significant warm bias over the upwelling cells when using such reprocessed SST products (Bensoussan et al. 2019). Using high-resolution ocean-atmosphere coupled modelling, Schaeffer et al. (2011) demonstrated that the small spatial scales of the wind are crucial to simulate properly ocean dynamics, including inertial oscillations and mesoscale variability such as upwelling in the north-western part of the GoL. However, atmosphere-ocean coupled modelling at high-resolution over the coastal ocean is still a very costly (e.g., high computational cost) and challenging (e.g., high resolution topography and forcing) task (Pairaud et al. 2011). *In-situ* observations from buoys, weather stations and moorings allow the study of small-scale processes, but these atmospheric and oceanic measurements are often sparse and suffer from limited temporal coverages. The present multi-sensor approach (O'Neill et al. 2012; Rossi et al. 2014) combines *in-situ* observations and model reanalysis complemented by remotely-sensed data to improve our understanding of coastal processes.

Benefiting from the long-term *in-situ* observations collected by the T-MEDNet collaborative network (T-MEDNet website) and a state-of-the-art climatic reanalysis at high spatio-temporal resolution, we are now able to revisit the scientific knowledge of these sporadic wind-driven coastal upwelling and downwelling events.

Here we develop a simple Wind-based Upwelling and Downwelling Index (WUDI) applied on ERA5-reanalysis winds, that was calibrated using *in-situ* temperature observations. It is used to create a database of wind-driven events along northwestern Mediterranean coastlines. Significant events per 20-km coastal cells are defined as transient vertical movements of water (upwelling/downwelling, resp.) resulting from wind-forced coastal divergence/convergence that lead to temperature changes (cooling/warming, resp.). WUDI approximates indeed the offshore/inshore Ekman transport per portion of coastline in accord with Ekman's seminal theory and its simplifying assumptions, which are thoroughly discussed (see also sect. 4.4). Our results show that the category of wind-driven events considered here effectively generate at specific locations measurable cooling or warming whose magnitude depends on the stratification. The statistical analysis of this events database allows identifying the main upwelling and downwelling coastal cells and describing their seasonal variability from monthly climatologies built over 1979-2019. Finally, we discuss our results against the literature and open perspectives for future research.

Table 1
Characteristics of the hourly *in-situ* temperature data collected by the T-MEDNet network at 11 sites (from northern Spain to Italy).

Site	First date	Last date	Available depths (m)	Longitude	Latitude
Medes	18-Jul-2002	04-Oct-2019	5; 10; 15; 20; 25; 30; 35; 40	3.23°E	42.05°N
Cap Creus	23-May-2007	29-Dec-2019	5; 10 ;15; 20; 25; 30; 35; 40	3.26°E	42.24°N
Banyuls	21-Mar-2006	26-Jul-2019	5; 10; 15; 20; 25; 30; 35; 40	3.17°E	42.47°N
Agde	26-May-2010	10-Nov-2020	10; 15; 20; 25; 30;	3.54°E	43.25°N
Carry-Le-Rouet	16-Jun-1997	14-Nov-2016	11; 23	5.16°E	43.32°N
Méjean	18-Jun-2010	16-Nov-2018	5; 10; 15; 20; 25; 30; 35; 40; 45	5.22°E	43.33°N
Marseille-Riou	24-Jun-1999	25-Nov-2019	5; 10; 15; 20; 25; 30; 35; 40	5.40°E	43.17°N
Cassis	14-Jun-2010	13-Jan-2020	5; 10; 15; 20; 25; 30; 35; 40; 45	5.56°E	43.02°N
Toulon-Cap Sicié	31-Jan-2014	17-Sep-2020	5; 10; 15; 20; 25; 30; 35; 40; 45; 50	5.84°E	43.04°N
Port-Cros	17-Jun-1999	24-Jul-2019	5; 10; 15; 20; 25; 30; 35; 40	6.38°E	43.15°N
Portofino	05-Jun-2015	17-Sep-2019	5; 10; 15; 20; 25; 30; 35; 40	9.17°E	44.31°N

2. Materials and Methods

2.1. Sea Surface Wind Data

Gridded Sea Surface Wind (SSW) products allow the study of the wind forcing at any point in space and time. Continuous grids can be obtained thanks to satellite data, which are often re-interpolated and/or gap-filled with information coming from other sources, or numerical models.

After pre-identifying 10 different gridded wind products, we retained the ERA5 reanalysis (Hersbach et al. (2020), downloaded on 22-Jun-2020) because its spatial resolution, temporal resolution and time coverage were the most suited for our study (Table SI-1). The data of reanalyses, such as ERA5, are model outputs that have been generated by assimilating satellite and *in-situ* observations corrected *a-posteriori* by merging multiple data sources.

2.2. *In-situ* temperature anomalies in the coastal ocean

The *in-situ* temperature data are long-term coastal observations collected following a standardized protocol by the T-MEDNet network. It was initiated more than a decade ago by Mediterranean marine ecologists to build a unified consolidated database of *in-situ* temperature in coastal waters (Bensoussan et al. 2010; Garrabou et al. 2019). T-MEDNet temperature time-series are recorded at hourly intervals, generally every 5 m from the surface to 40 m depth (or more) using similar data loggers (thermistors of 0.21°C accuracy that are attached on the seabed). Sustained field monitoring was complemented by the launch, in 2009, of a collaborative online platform (T-MEDNet.org) for rigorous data quality check, management and long-term storage.

This database is particularly well suited for the analysis of the high-frequency variability of the temperature in the coastal waters and several monitoring sites are located in known or previously established up/downwelling zones. After an evaluation of the data coverage and continuity of all available observations, pluri-annual nearly continuous time-series of seawater temperatures (main characteristics are displayed in Tab. 1) from 11 sites (Fig. 1) were retained in our study.

To detect upwelling and downwelling processes through their associated temperature anomalies, two specific depths are considered, as in Rossi et al. (2014). For the upwelling detection, the 10m deep temperature is used, while the 35m deep temperature (generally below the summer thermocline, as reported by Bensoussan et al. (2010)) is used for the downwelling detection. For more details refer to Table 1. Due to sensors' problems and/or maintenance operations, in-situ data are sometimes lacking at the target depth; data-gaps are minimal, concerning in average 1.5 % (from 0.5 % to a maximum of 5 %) of the total duration of the time-series. In these cases, vertical interpolation is performed between the nearest vertical observations (i.e. 5/15 m for the surface temperature; 30/40 m for the subsurface temperature), when available; otherwise, missing values are kept.

To capture best the thermal signatures of wind-driven events at each site, we analyze high-frequency temperature anomalies that are obtained by subtracting low-pass filtered signals (containing only periods higher than a prescribed value) from the raw temperature time-series. Following Rossi et al. (2014), in agreement with the mean duration and frequency of occurrence of these intermittent processes (Jacq et al. 2005), the cut-off period of the filter is set to 15 days. As such, low frequency (e.g. monthly, seasonal, annual, inter-annual) variations are removed from the final signals that contain only the high-frequency variability of ocean temperature. Positive anomalies at 35m represent warming events due to downwelling while negative anomalies at 10m symbolize cooling events due to upwelling.

Note that tidal effects have been neglected here since the Mediterranean Sea is considered as a micro-tidal system. Both tidal-induced currents and potential associated temperature changes are indeed very weak in the northwestern basin (Ferrarin et al. 2018), especially in the GoL and the Ligurian Sea where they are hardly detectable and chaotic (Alberola et al. 1995).

2.3. Wind-based Upwelling and Downwelling Index (WUDI)

2.3.1. Ekman Transport Formula and Projection

The Wind-driven Upwelling-Downwelling Index retained here is the "Bakun Index" (Bakun 1975; Bakun 1973) modified following (Alvarez et al. 2011; Rossi et al. 2014; Jacox et al. 2018). By integrating the reduced equations of motions (to a balance between the Coriolis and frictional forces, under Ekman assumptions) from a depth where internal stresses vanish (i.e. Ekman depth d_E) to the surface gives relationships for volume transports per unit of length as a function of wind stress (Eq. 1). The vertical structure of the horizontal motions (assuming a constant vertical viscosity) is the Ekman spiral: it predicts an integrated near-surface transport directed 90° to the right (left, resp.) of the surface wind stress in the northern (southern, resp.) hemisphere. The water displaced offshore (inshore, resp.) must be compensated from "below" (from "above", resp.) due to the presence of the nearby coast. As such, the wind-driven Ekman transport projected onto the main coastline direction (Eq. 2) is equal to the upward (positive WUDI) or downward (negative WUDI) vertical transport into the Ekman layer, thus constituting a good proxy for coastal upwelling and downwelling processes.

Horizontal Ekman transport is calculated from gridded 10m SSW data $W(W_x, W_y)$ as the wind-induced horizontal transport perpendicular to the coastline, positive in the offshore direction. The zonal and meridional components Q_x and Q_y are computed as :

$$Q_x = \frac{\rho_A C_d}{f \rho_w} \|W\| W_y \text{ and } Q_y = -\frac{\rho_A C_d}{f \rho_w} \|W\| W_x \quad (1)$$

With $\|W\| = \sqrt{W_x^2 + W_y^2}$, $\rho_A = 1.22$ kg.m^{-3} (air density), $\rho_w = 1024$ kg.m^{-3} (water density), C_d a dimensionless drag coefficient $C_d = 1,1 \times 10^{-3}$ when $\|W\| < 6$m.s^{-1}, or $C_d = (0.61 + 0.063\|W\|) \times 10^{-3}$ when $\|W\| \geq 6$m.s^{-1}, $f = 2\Omega sin(\phi)$ (Coriolis parameter) with $\Omega = 7.2921158 \times 10^{-5}$ rad.s^{-1} (Earth angular velocity) and ϕ the latitude.

WUDI is finally defined as the integrated shore-normal Ekman transport per meter of coastline (Bakun 1973), indicating offshore transport if WUDI>0 (upwelling favorable), or onshore transport if WUDI<0 (downwelling favorable):

$$WUDI = Q_\perp = Q_x \cos(\alpha) - Q_y \sin(\alpha) \quad (2)$$

The clockwise angle α is the angle between the vector pointing northward and the direction of the coastline. See Figure 1 of Supporting Information for visual representation of α. Note also that the WUDI formula (Eq. 1 and 2) returns projected wind-induced Ekman transport values that are already integrated over the Ekman depth d_E, despite the fact that it does not intervene explicitly in the formulation.

Examining the validity of all theoretical assumptions behind the use of Ekman's theory to describe flow in the surface boundary layer of the coastal ocean (Stewart 2008) (see section 9.2, p. 141) is beyond the scope of this applied statistical study. Nevertheless, the "deep water", "steady state" and "vertical diffusivity" assumptions raise questions that are discussed later on (sect. 4.4). The "no boundaries" assumption, stating that Ekman theory is mainly valid away from coasts, has been largely questioned in the last decades with the numerous applications of Bakun's inspired indices that successfully explain the variability of both temperature and nutrient in many coastal systems (Bakun 1975; Alvarez et al. 2011; Rossi et al. 2014; Jacox et al. 2018). Here we retain this largely used and robust index as a simple tool to investigate the variability of up/downwelling favorable events at the scale of 20-km coastal segments, even though the theory might not be entirely respected. Despite the fact that this simple index is an incomplete representation of the full physics driving coastal circulation and upwelling, it has been shown to capture well intermittent wind-driven coastal processes and their thermal responses. Therefore, while it may not represent the true effect of the wind on the coastal ocean, it provides a good representation of upwelling/downwelling events that result from transient wind-driven coastal divergence/convergence.

2.3.2. Potential Up/Downwelling Cells

In agreement with the spatial scales of coastal upwelling cells described by Millot and Wald (1981) and Millot (1990), the Northwestern Mediterranean coastlines extracted from the Global Self-consistent, hierarchical, high-resolution shoreline database (Wessel and Smith 1996) are discretized in contiguous 20-km segments. We developed an automatic algorithm, complemented by tailored hand-made adjustments for 10% of the points, to obtain the coastline orientation and mean geographic position for 55 segments. The wind forcing associated with the portion of coastline is obtained using spatial weighted interpolation considering only the neighboring ERA5 grid points falling over the sea while discarding land-points (Figure SI-1).

Those coastal 20-km segments are hereafter referred to as potential "cells" where downwelling and/or upwelling events are expected to occur.

2.4. Statistical relationships between wind-forced up/downwelling events and their Thermal Responses

2.4.1. Delayed oceanic responses

Rossi et al. (2014) showed that the coastal temperature changes occur slightly after the initiation of favorable wind-forcing. To study these typical delays in the region, we calculate lagged cross-correlations between both WUDI and temperature anomaly time-series at each of the 11 *in-situ* T-MEDNet sites. Prior to the correlations, we apply a 6-hour moving average and subsequent sub-sampling to the hourly 10m and 35m temperature anomaly time-series to match the WUDI time-series temporal resolution. Then, the correlation coefficients and slopes of the linear regressions of time-series of WUDI and sub-sampled 10m or 35m temperature anomalies are calculated for each site, applying different time

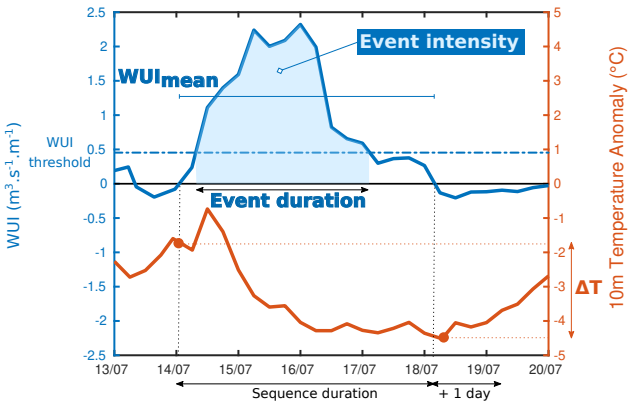

Figure 2: Schematic representation of the 2-step procedure using WUDI sequences to determine a statistical threshold selecting the most significant events, taking the July-2012 upwelling event as an example (Fig. 1). The blue line represents the 6-hourly WUDI index while the red line is the 6-hourly 10m temperature anomalies measured at Cassis over July 13-19, 2012. The vertical black dotted lines indicate the sequence duration (i.e. consecutive days with positive WUDI, 5 days in this case). ΔT is defined as the initial temperature anomaly minus the most extreme anomaly (here the minimum) attained during the sequence duration extended by one day (to capture delayed responses). The horizontal dotted blue line is the WUDI threshold (75^{th} percentiles of the mean WUDI values recorded during all sequences and at all sites) capturing only the most significant upwelling events. In this case, the recorded event lasts only 2.75 days, which is the period during which WUDI index exceeds the threshold.

lags (between -5 days and +5 days, using intervals of 6 hours); the typical response time is then inferred from the maximum correlation coefficient R.

2.4.2. *Defining WUDI thresholds by selecting the most significant events*

The objective of this part is to define quantitatively the category of events that are going to be considered in this study, both by WUDI values (relative to the wind forcing), and water temperature variation (relative to the oceanic response). We aim at describing the occurrence of the most significant wind-forced events, defined here as all upwelling or downwelling events that effectively trigger quantifiable cooling or warming at any coastal cell.

Simple approaches (not shown) were not satisfactory since the relationships between WUDI and observed temperature time-series are very complex (see also Section 3.1) and site-specific. For instance, the time it takes for the temperature to decrease varies from site to site (see also sect. 2.4.1 and Tab. 2). Moreover, previous studies (Rossi et al. 2014) and preliminary analyses highlighted that the most extreme anomalies can be attained either during the period of favorable wind-forcing or slightly after, when calm conditions allow relaxation (Fig. 2).

To determine generic WUDI thresholds defining these most significant wind events, we propose a 2-step statistical procedure. First, we define the upwelling (downwelling, respectively) favorable periods as consecutive sequences of strictly positive WUDI (strictly negative, respectively). Given the pulse wind regimes in the Mediterranean Sea, successive sequences separated by a wind–reversal lasting less than one day are merged into a single sequence. Then, for each sequence and site, we calculate the corresponding temperature changes (ΔT) by computing the difference between the 10m (35m, respectively) temperature anomaly measured at the beginning of the sequence (when the favorable wind just starts blowing) and the minimal (maximal, respectively) temperature anomaly attained during the WUDI sequence prolonged by 1 day, to allow capturing delayed maximal responses.

Each upwelling (downwelling, resp.) favorable WUDI sequence is characterized by its initial date, duration, mean value and ΔT (Fig. 2). We choose the conservative approach of only considering the most intense events for this study. Instead of an empirical approach, we define these extreme events based on the 75^{th} percentile of the mean WUDI, that are the 25% strongest up/downwelling favorable wind sequences for the duration of the sequence. After aggregating the mean WUDI values from all favorable sequences pooled together for the 11 sites, we calculate the mean WUDI values separating the 25% most intense sequences from the rest (i.e. those constituting the 4^{th} quartile) to obtain a negative WUDI threshold for downwelling on one hand, and a positive WUDI threshold for upwelling on the other hand. The medians of the temperature variations induced by these extreme favorable sequences are kept to give an order of magnitude of the oceanic response for the considered category of events.

From now on and everywhere in the manuscript, we define upwelling (downwelling, respectively) events as discrete time periods characterized by a WUDI index greater (lower, respectively) than the corresponding threshold.

Two databases are created for the entire coastlines of interest: one for upwelling events and one for downwelling events, using the WUDI thresholds corresponding to the 25 % most intense sequences. Each event is characterized by its initial date, its location, its duration and its intensity (WUDI integrated over the event duration, see also Fig. 2). From these event databases, the mean number of up/downwelling favorable days per month (d.mo^{-1}) for each coastal cell is determined by averaging the durations of all the significant events that started during a given month over the 40-year period spanning 1979-2019.

To test the sensitivity of our results to the statistical thresholding procedure, note that we also reported monthly statistics of *extreme events* using the WUDI thresholds corresponding to the 5 % most intense sequences. Additionally, we compute the mean predicted Ekman transport (quantity of water integrated over the Ekman depth that is horizontally transported due to the wind forcing) for each month and each cell in a similar manner but using the WUDI integral over the event's duration (illustrated in Fig. 2), instead of the duration (Section SI-5). The former methodology tends to give

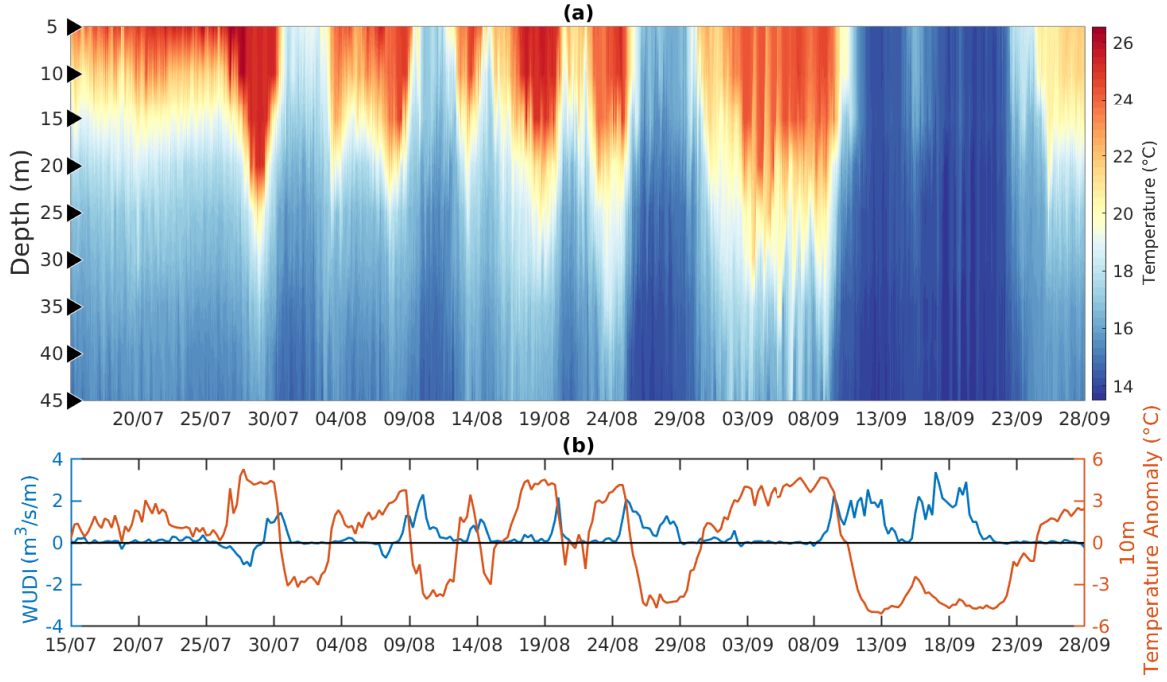

Figure 3: Vertical temperature profile, WUDI index and 10m temperature anomaly time-series off Cassis during an exemplary ~2.5-month stratified period (from 15-Jul-2013 to 28-Sep-2013). (a) *in-situ* temperatures measured at 9 depths (black triangles, see also Table 1). (b) 10m temperature filtered anomalies (°C, red line) and WUDI index computed from ERA5-SSW ($m^3.s^{-1}.m^{-1}$, blue line).

more importance to the duration of the wind-forcing, independently of its intensity (as soon as it is greater than the threshold); conversely, the latter one evaluates together both event's duration and intensity.

2.4.3. Categorizing the thermal responses

Given the strong seasonality of the upper-ocean stratification in our study area (D'Ortenzio et al. 2005) the oceanic temperature response to atmospheric forcing is expected to be maximum in summer, during the period of strong and shallow thermal stratification, but hardly detectable in late winter, when the water column can be fully mixed. This probably explains why most upwelling studies to-date have focused essentially on the summer season (Millot 1979; Pinazo et al. 2018) despite the fact that strong favorable forcing also occur during winter (Bakun and Agostini 2001; Jacq et al. 2005). Moreover, D'Ortenzio et al. (2005) also documented substantial inter-annual variability of the Surface Mixed-Layer (SML) so that the "stratified" period does not concern exactly the same period each year.

Here, we intend to evaluate the temperature response to wind forcing under different ocean stratification states. Hence, for each monitoring sites, we define "stratified" and "unstratified" periods by evaluating the low-pass-filtered 10m temperature time-series as compared to its total mean value (Sect. 2.2). More specifically, "stratified" periods are defined when the corresponding filtered temperature is above the mean, otherwise, it is qualified as an "unstratified" period (see Fig. SI-2, SI-3, SI-4 and SI-5). This simple approach highlights significant inter-annual variability in the duration and extension of the annual stratified periods, which would not have been properly addressed using calendar/seasonal criteria.

All significant events constituting our databases (Sect. 2.4.2) are then clustered in both event categories (i.e. up/downwelling) for subsequent analysis of associated ocean temperature changes. By pooling all events from all sites into both categories, we can then analyze the statistical distribution of the coastal temperature responses to both up/downwelling events during the stratified and unstratified periods.

3. Results

3.1. Validation of WUDI using Observational Temperature Time-Series

We investigate the thermal responses of the upper coastal ocean to sporadic wind-driven events by focusing on two contrasted sites, Banyuls and Cassis, which were shown to be prone to frequent downwelling and upwelling, respectively (Millot 1979; Millot 1990; Bakun and Agostini 2001). For each site we analyze exemplary periods characterized by both stratified (Fig. 5 and 3) and unstratified (Fig. 6 and 4) conditions. Note that these joint analyses were also conducted for the other 11 monitored sites (not shown), leading to similar conclusions.

Off Cassis, short-lived (a few days to a week or more) cooling events repeatedly (5-6 times) occur over 2 exemplary summer months (Figure 3), that is when the stratifi-

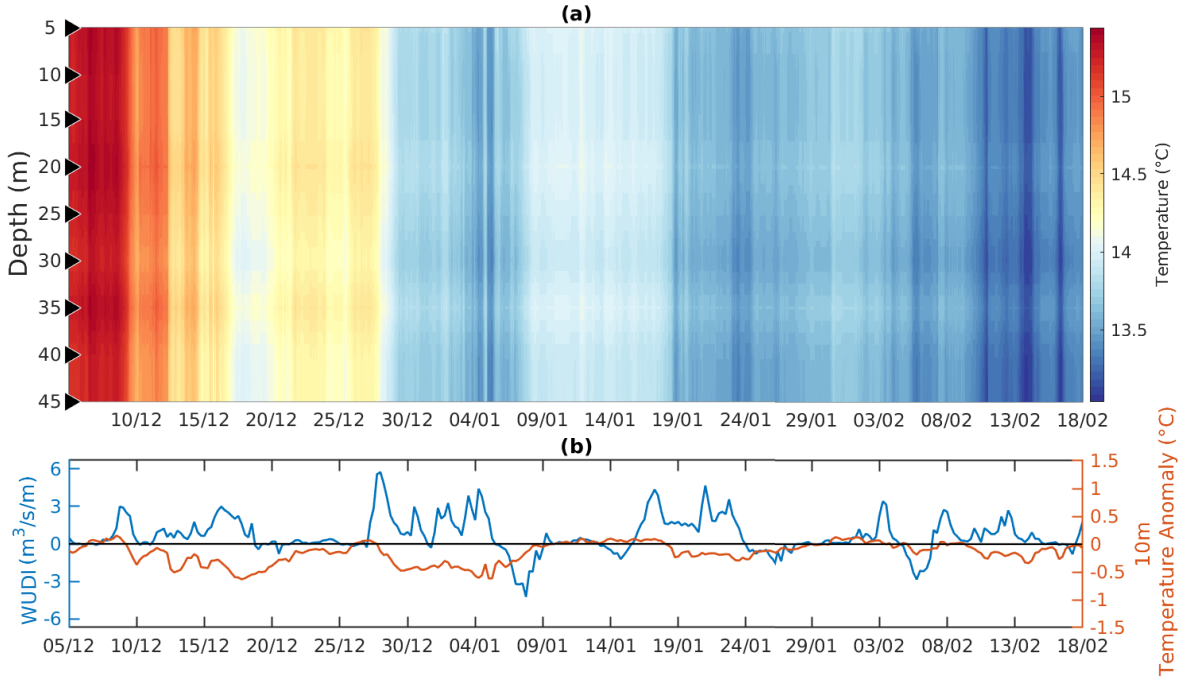

Figure 4: Vertical temperature profile, WUDI index and 10m temperature anomaly time-series off Cassis during an exemplary ∼2-month unstratified period (from 05-Dec-2016 to 18-Feb-2017). (a) *in-situ* temperatures at 9 depths (black triangles, see also Table 1). (b) 10m temperature filtered anomalies (°C, red line) and WUDI index computed from ERA5-SSW ($m^3.s^{-1}.m^{-1}$, blue line).

cation is strong with temperatures ranging 13.5-26.5°C in the top 50 m. Under stratified conditions, both time-series suggest a tight inverse relationship between the wind forcing and the thermal response (Fig. 3b) : positive WUDI sequences match negative temperature anomalies indicative of upwelling events. For example, the episode of 25-30 August 2013 displays a -6°C temperature drop occurring over 5 days when the wind forcing is particularly favorable for upwelling (WUDI ∼ 1.5 $m^3.s^{-1}.m^{-1}$, Fig. 3b). The strongest and longest event lasts about 12 days (9-21 September 2013) and shows that water may ascend from depths far below 45m (Fig. 3(a)), inducing a surface temperature drop of ∼11°C (from 25°C to 14°C) for more than two weeks (except during a weak superficial warming on 15-16 September related to a short mistral relaxation). It is worth noting that even short upwelling favorable wind events can trigger significant oceanic responses, like the one-day episode spanning 29-30 July 2013, for which the negative temperature anomaly occurs after the end of the wind forcing (Fig. 3b). Overall, short delays are noticeable between the onset of upwelling-favorable wind forcing and the actual surface signatures of the cooling events, as exemplified by the event starting on 29 July 2013.

Note also that downwelling favorable conditions associated with a deepening of the 20°C isotherm and a relative warming of the coastal ocean do occur sometimes (i.e. 25-28 July 2013) off Cassis.

Despite highly positive WUDI (upwelling-favorable) during winter off Cassis (Fig. 4), the associated drops of ocean temperatures are obviously less marked than during the stratified periods. For instance, the long and intense episode of upwelling-favorable forcing occurring from 27 December 2016 to 5 January 2017, with WUDI reaching up to 6 $m^3.s^{-1}.m^{-1}$, is associated with a relative surface cooling of only -0.5°C (Fig. 4b).

Despite strong vertical stratification (temperatures span 14-23°C in the top 50 m), a striking feature revealed by the temperature profiles off Banyuls is the frequent occurrence of warming events (4 to 9 events) over the 2 summer months (Fig. 5a). They are of short duration (few days) but of great intensity, with temperatures measured at 30-40m exceeding 20°C (Fig. 5a) and corresponding positive 35m temperature anomalies (Fig. 5b) due to the deepening of the mixed layer associated with wind-driven downwelling.

For example, a WUDI index reaching -1.7 $m^3.s^{-1}.m^{-1}$ during the episode from 09-Aug to 12-Aug 2016 is associated with a deepening of the 20°C isotherm and a relative warming of +4°C.

For most of the warming events, a short delay between the onset of the downwelling favorable conditions and the temperature increase at ∼35m is observed. For instance, a delay of 1,5 day is noticeable for the downwelling episode of mid-July 2016.

While Banyuls is used here to exemplify the thermal responses of downwelling events, it also rarely experiences upwelling-favorable conditions (positive WUDI, such as over 17-19 July 2016 and 12-14 september 2016) that are associated with relative cooling of the coastal ocean and subse-

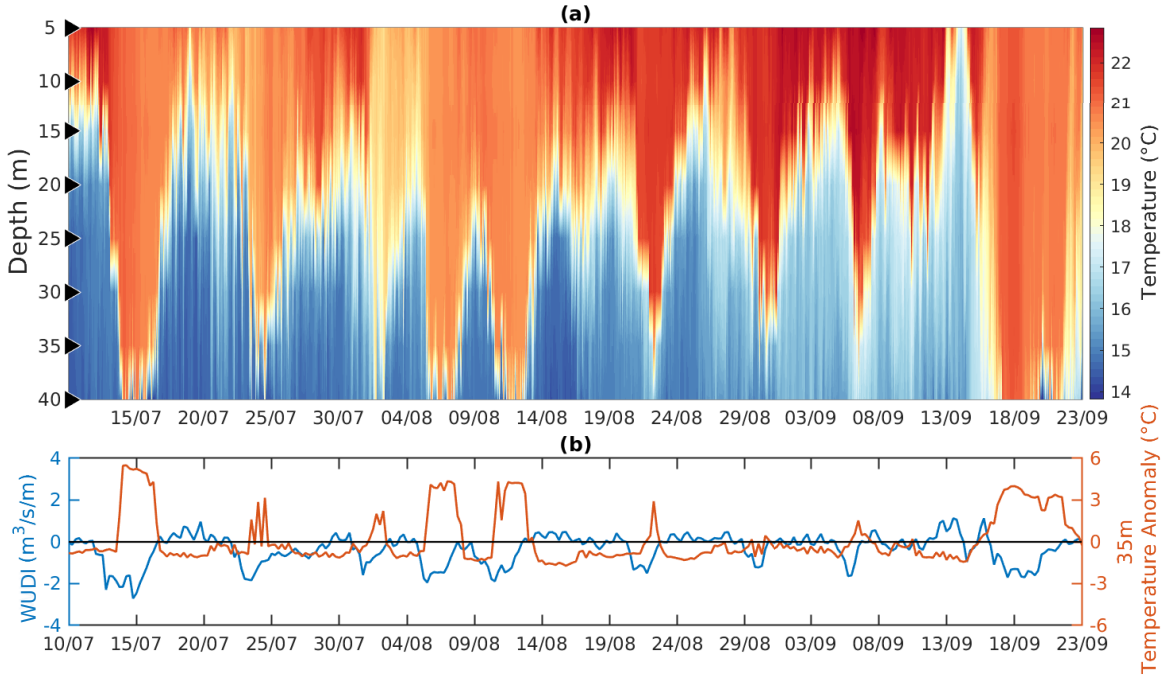

Figure 5: Vertical temperature profile, WUDI index and 35m temperature anomaly time-series off Banyuls for an exemplary ~2-month stratified period (from 10-Jul-2016 to 23-Sep-2016). (a) *in-situ* temperatures measured at 8 nominal depths (black triangles, see also Table 1). (b) 35m temperature filtered anomalies (°C, red line) and WUDI index computed from ERA5-SSW ($m^3.s^{-1}.m^{-1}$, blue line)

quent uplift of the thermocline to shallower depths.

During unstratified period (Fig. 6), coastal temperatures only span 9.5-13°C, exemplifying small vertical gradients between 5 and 35m. The maximum intensity of the wind-forcing in winter (reaching more than -5 $m^3.s^{-1}.m^{-1}$, Fig. 6b) is higher than during stratified period (-2.5 $m^3.s^{-1}.m^{-1}$, Fig. 5b). However, the thermal response does not scale with the extreme WUDI intensity because the water column temperature is more homogeneous. For example, the extreme WUDI value of -4 $m^3.s^{-1}.m^{-1}$ characterizing the event of the 5-10 February 2013 corresponds to a relative warming at 35m of +1°C. For other years and other sites, typical responses span 0.5-1.5°C (not shown), which remain significant considering the sensors specifications (about 0.2°C accuracy, 0.02°C resolution, (Bensoussan et al. 2010; Bensoussan et al. 2019). Note that a few periods dominated by downwelling-favorable wind forcing (i.e. 23-27 February 2013) do not coincide with a relative subsurface (35m) warming probably because it occurred simultaneously with a regional convection event associated with dense water formation over the shelf (Bourrin et al. 2008) and offshore, leading to homogeneous and extremely low (~ 10°C) temperatures (Houpert et al. 2016).

Altogether, these analyses highlight the tight relationship between intermittent wind forcing and rapid changes of coastal thermal characteristics associated with the vertical dynamics of the thermocline. It reveals that the high frequency variability of coastal temperatures appears largely determined, although often with a slight temporal delay, by the transient up/downwelling favorable wind events, which may occur at any time of the year and at various sites. It finally illustrates two "regimes" of thermal responses linked to the intra-annual variability of the upper stratification in the Mediterranean Sea.

3.2. Statistical Regressions to Define Typical Ocean Temperature Responses

3.2.1. Temporal and Spatial Mismatch of Temperature Response to Sporadic Wind-Forcing

We now investigate the delay between the maximum thermal response and the wind-forcing, previously exemplified in Section 3.1, for all up/downwelling events using lagged correlations for all available surface and subsurface *in-situ* time-series.

Ekman theory predicts that a positive WUDI (upwelling favorable) is associated with negative surface temperature anomalies (cooling of surface layers), and that a negative WUDI (downwelling favorable) is associated with positive subsurface temperature anomalies. With our conventions, all correlations reported in Table 2 are negative because the temperature anomalies and the WUDI values are of opposite signs for both upwelling and downwelling processes.

It suggests that, for the complete time-series, the typical delays for the maximum thermal responses to appear after favorable winds range from 6 to 54 hours (mean = 27 hours) for upwelling while they span 12-66 hours (mean = 32 hours) for downwelling. For instance, the Cassis upwelling is characterized by a lag of 1.5 days (36 hours) while cooling

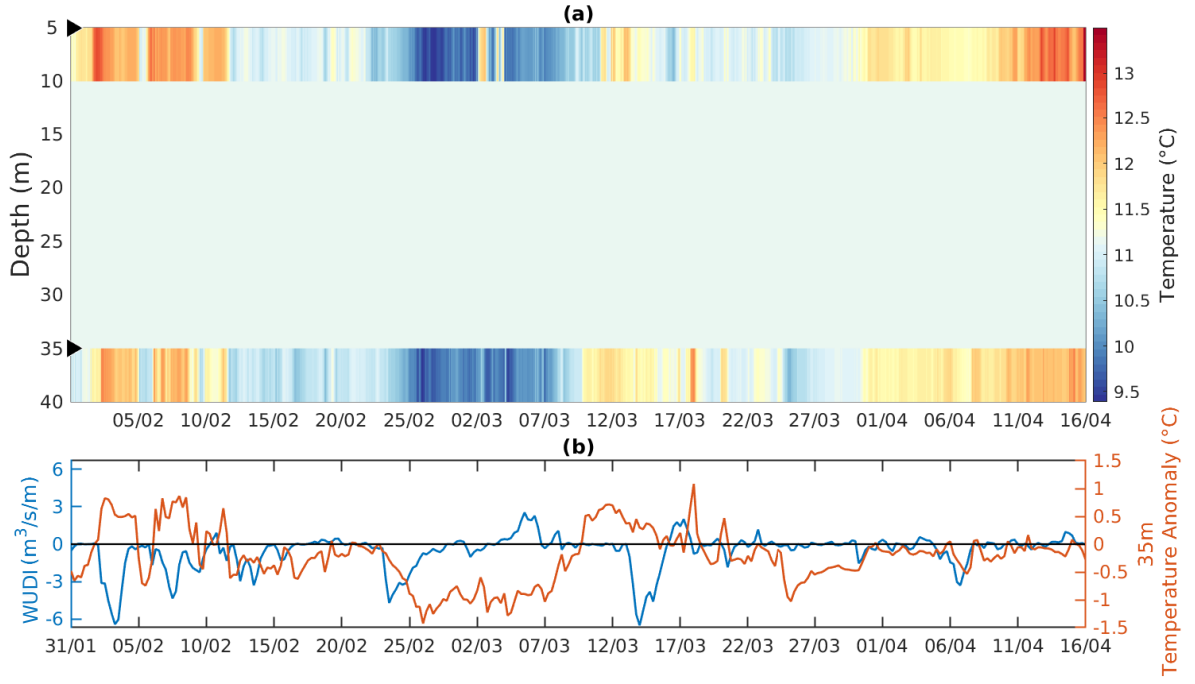

Figure 6: Vertical temperature profile, WUDI index and 35m temperature anomaly time-series off Banyuls for an exemplary ~2.5-month unstratified period (from 31-Jan-2013 to 16-Apr-2013). (a) *in-situ* temperatures measured at 2 depths (black triangles, see also Tab. 1). (b) 35m temperature filtered anomalies (°C, red line) and WUDI index computed from ERA5-SSW ($m^3.s^{-1}.m^{-1}$, blue line).

Table 2
Lagged cross-correlation coefficients (R) and corresponding temporal lag of WUDI Versus 10m and 35m Temperature anomalies at 11 T-MEDNet sites over the whole periods of availability (left hand-side; see also Tab. 1) and during summer months (June, July, August, September) only (right hand-side).

	Entire Time-Series		June to September	
	WUDI versus 10m Temperature anomaly	WUDI versus 35m Temperature anomaly	WUDI versus 10m Temperature anomaly	WUDI versus 35m Temperature anomaly
Medes	-0.03 (-0.25 d)	-0.16 (-1 d)	-0.32 (-0.5 d)	-0.51 (-1 d)
Cape Creus	-0.08 (-0.25 d)	-0.18 (-0.5 d)	-0.20 (-0.25 d)	-0.39 (-0.5 d)
Banyuls	-0.06 (-0.25 d)	-0.20 (-0.5 d)	-0.31 (-0.25 d)	-0.56 (-0.5 d)
Agde	-0.28 (-2.25 d)	-0.27 (-2.75 d)	-0.41 (-2.25 d)	-0.34 (-2.75 d)
Carry-Le-Rouet	-0.30 (-1.5 d)	-0.33 (-2 d)	-0.53 (-1.5 d)	-0.54 (-2 d)
Méjean	-0.28 (-1.5 d)	-0.33 (-2 d)	-0.53 (-1.5 d)	-0.54 (-1.75 d)
Marseille-Riou	-0.34 (-1.25 d)	-0.37 (-1.25 d)	-0.61 (-1.25 d)	-0.56 (-1.25 d)
Cassis	-0.33 (-1.5 d)	-0.38 (-1.25 d)	-0.61 (-1.25 d)	-0.58 (-1 d)
Toulon-Cap Sicié	-0.30 (-0.75 d)	-0.37 (-0.75 d)	-0.55 (-0.5 d)	-0.57 (-1 d)
Port-Cros	-0.15 (-1.75 d)	-0.23 (-1.25 d)	-0.38 (-1.5 d)	-0.41 (-0.5 d)
Portofino	-0.10 (-1.25 d)	-0.13 (-1.5 d)	-0.22 (-1.25 d)	-0.28 (-1.5 d)

All correlations are significant to the 95% confidence level

at Toulon Cap-Sicié occurs with an average lag of 0.75 day (18 hours) after favorable forcing. The maximum warming due to downwelling events are measured with lags of 0.5 day (12 hours) at Banyuls, 2 days at Méjean and 1.25 days (30 hours) at Marseille-Riou.

In summertime, the portion of coast between Méjean and Toulon shows the strongest correlations between upwelling-favorable wind forcing and surface ocean response, with Cassis and Marseille Riou displaying the tightest correlations (R=-0.61), while the mean lag for upwelling along this coastline is 28 hours. Overall, the shortest lags are found at Banyuls and Cape Creus (6 hours), followed by Medes and Toulon Cap Sicié (12 hours). The longer lags appear at Agde (54 hours), then along "Côte Bleue" (Mejean, Carry-le-Rouet) and Port-Cros (36 hours) and finally at Cassis/Marseille-Riou (30 hours). The tight lagged correlations found during summer at Cassis/Marseille Riou suggest that 37% (R^2) of the 10m temperature variability is explained by WUDI.

During summer, the coastlines from Medes to Toulon Cap Sicié also present tight correlations between downwelling

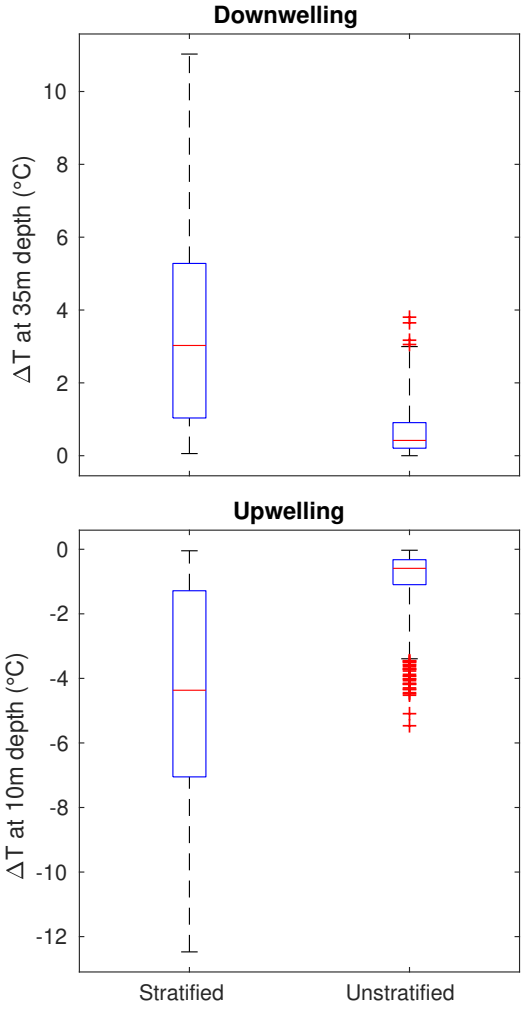

Figure 7: Boxplots of the typical oceanic temperature responses for both downwelling (upper panel, at 30 m) and upwelling (lower panel, at 10 m) significant events (i.e. mean WUDI surpassing the statistical thresholds reported in Tab. 4), as a function of the stratification regime (left: stratified conditions; right: unstratified conditions). All data from the 11 T-MEDNet sites were used. The whiskers are determined with a value W=3, the outliers are values larger than $Q_3+W(Q_3-Q_1)$ or smaller than $Q_1-W(Q_3-Q_1)$, with Q_1 the 1^{st} quartile and Q_3 the 3^{rd} quartile.

favorable winds and 35m temperature anomalies, with maximum values found at Marseille Riou, Cassis and Toulon Cap Sicié (R=-0.56 to -0.58) as well as at Medes and Banyuls (R=-0.51 to -0.56). The latest findings suggest that 31% and 34% (R^2) of the 35m temperature variability is explained by WUDI at Banyuls and Cassis, respectively. The mean lag for downwelling along this portion of coast is 34 hours. Overall, response lags for summer downwelling events range from 12 hours (at Port-Cros, Banyuls and Cape Creus) to 66 hours at Agde with intermediate delays of 24-30 hours at Cassis and Marseille-Riou or 42-48 hours along "Côte Bleue" (Mejean, Carry-le-Rouet).

Overall, our results indicate that the relationships between favorable winds and delayed thermal responses vary largely between the 11 monitored sites, thus preventing us to derive a single statistical relationship valid for all the cells pertaining to the studied coastlines. It also suggests that the intensity of the thermal response is variable from site to site, as shown by the site-specific median thermal responses to favorable WUDI sequences reported in Table 3.

Overall for all sequences, it shows that the mean thermal anomalies are about 5 times higher during stratified period than during unstratified period (about 6 times, for the top 25% sequences). During stratified periods (see also Fig. SI-2 to SI-5), the coastline displaying the most intense 10m cooling associated with the top 25% upwelling favorable WUDI sequences covers Agde to Port-Cros with medians ranging from -2.00°C at Port-Cros to -5.63°C at Méjean and Marseille Riou. For stratified conditions, the coastline exhibiting the most intense 35m warming related to the 25% strongest downwelling favorable WUDI sequences encloses from Medes to Agde with medians ranging from 2.09°C at Cape Creus to 2.73°C at Medes.

3.2.2. *Definition of WUDI Thresholds to define Significant Wind-Driven Events and to quantify their Associated Thermal Responses*

The WUDI thresholds, defined as the 75^{th} percentile of the mean WUDI intensity of all WUDI sequences of all temperature monitoring sites, are +0.45 $m^3.s^{-1}.m^{-1}$ for upwelling and -0.35 $m^3.s^{-1}.m^{-1}$ for downwelling (Tab. 4). The corresponding alongshore wind speed values are 5.84 $m.s^{-1}$ for upwelling and 5.15 $m.s^{-1}$ for downwelling.

The corresponding temperature responses measured at all monitoring sites for the 25% WUDI sequences with highest mean WUDI exhibit substantial variability clearly visible on the boxplots (Fig. 7). Both the medians (red bars, also reported in Tab. 4) and the statistical distributions highlight the importance of treating separately the thermal responses as a function of the stratification regime. Both absolute cooling and warming medians are approximately one order of magnitude higher during stratified periods as compared to unstratified periods (Tab. 4). The highest variability is observed during the warm stratified periods, with extreme values of surface (10m) cooling of up -12.5°C for upwelling and subsurface (35m) warming of +11°C for downwelling, in comparison to -5°C and +4°C for the unstratified boxplots.

These WUDI thresholds, which are applied on the whole surveyed coastlines, are used to define a category of significant up/downwelling events that have quantifiable thermal signatures of variable intensity depending on the water column stratification (Tab. 4). A global wind-based event analysis is conducted to determine the frequency of occurrence and the intensity of the up/downwelling events along northwestern Mediterranean coastlines.

Table 3
Median 10m/35m ΔT taking into account all upwelling/downwelling favorable WUDI sequences and only the 25% strongest sequences, for all the *in-situ* temperature sites, as a function of the stratification regime.

	Median 10m temperature response for upwelling episodes (°C)				Median 35m temperature response for downwelling episodes (°C)			
	25% extreme sequences		All sequences		25% extreme sequences		All sequences	
	Stratified	Unstratified	Stratified	Unstratified	Stratified	Unstratified	Stratified	Unstratified
Medes	-1,05	-0,18	-0,63	-0,14	2,73	0,32	1,41	0,20
Cape Creus	-0,98	-0,20	-0,66	-0,14	2,09	0,17	2,26	0,17
Banyuls	-1,29	-0,34	-0,62	-0,19	2,38	0,42	1,10	0,31
Agde	-2,90	-0,99	-1,16	-0,35	2,16	0,40	0,51	0,22
Carry-Le-Rouet	-5,08	-0,81	-1,05	-0,37	1,56	0,32	0,67	0,22
Méjean	-5,63	-0,52	-0,75	-0,21	1,52	0,19	0,69	0,12
Marseille-Riou	-5,63	-0,54	-0,94	-0,17	1,75	0,16	0,76	0,14
Cassis	-4,33	-0,48	-0,91	-0,15	1,74	0,15	0,70	0,13
Toulon-Cap Sicié	-4,98	-0,55	-0.86	-0,18	1,29	0,18	0,86	0,15
Port-Cros	-2,00	-0,23	-0,62	-0,12	1,60	0,09	0,92	0,10
Portofino	-0,81	-0,29	-0,42	-0,18	1,75	0,23	0,48	0,13

Table 4
WUDI universal thresholds, corresponding alongshore wind speeds and median temperature responses (at 35m for downwelling and at 10m for upwelling) of the extracted 25% strongest wind forcing sequences, as a function of the stratification regime.

	WUDI thresholds	Corresponding alongshore wind	Median ocean temperature response	
			Stratified	Unstratified
Upwelling	+0.45 $m^3.s^{-1}.m^{-1}$	5.84 $m.s^{-1}$	-4.37°C	-0.59°C
Downwelling	-0.35 $m^3.s^{-1}.m^{-1}$	5.15 $m.s^{-1}$	+3.03°C	+0.42°C

3.3. Statistical Occurrence of Wind-Driven processes along the North-Western Mediterranean coastlines

Using the WUDI thresholds defined previously (25% most intense sequences), a database of discrete events is constructed for the entire study area at 20 km resolution considering the 1979-2019 period. From this database of favorable events triggering significant responses, monthly climatologies of upwelling (Fig. 8) and downwelling (Fig. 9) events are calculated for all cells (N=55) along the North Western Mediterranean shores. The y-axis of the monthly Hövmoller diagrams starts in June and ends in May for visual purposes.

The mean number of days favorable for up/downwelling varies between 0-13 days per month ($d.mo^{-1}$). For both processes, the mean number of events per month per potential cell is greater during winter-spring (November to April) than during summer-autumn (May to October). For upwelling, 2 to 3 events occur in winter-spring as compared to a mean of 2 events in summer-autumn (Fig. 8c); it is slightly more marked for downwelling with about 2-3 events in winter-spring and only 1 to 2 events in summer-autumn (Fig. 9c).Overall, 58% (resp. 64%) of the total upwelling (resp. downwelling) favorable wind forcing occur during winter-spring, the remaining take place during summer-autumn. Concerning the annual statistics (Fig. 8b and 9b), note that the total number of daily event per year slightly decreases (exemplifying the scarcity of extreme events) while the main alongshore variability is maintained (attesting the robustness of our results) when considering the 5 % most intense sequences (black lines) instead of the strongest 25 % (blue lines).

To ease the analysis of our results, our study region is subdivided into 4 different sections mimicking the sharp changes of orientation of the shorelines (see white dotted line on Fig. 1 and the black dotted lines on Fig. 8 and 9), from West to East: W-GoL, E-GoL, W-Lig, E-Lig.

W-GoL : Medes to Narbonne

This coastline constitutes the most prominent downwelling zone of the North-Western Mediterranean basin. Downwelling events occur from 4 to 13 $d.mo^{-1}$ during November-April, with a local maximum at Banyuls. From May to October the number of favorable days spans 2-10 $d.mo^{-1}$. The two main downwelling cells are Banyuls and Medes, with downwelling-favorable wind conditions occurrence reaching respectively 130 and 100 days per year ($d.y^{-1}$) on average over the 1979-2019 period (Fig. 9b).

This zone is also characterized by upwelling-favorable winds occurring at any time of the year but relatively rarely, spanning 0-5 $d.mo^{-1}$, with a mean of 30 upwelling $d.y^{-1}$ over this coastal section, and a maximum of 50 $d.y^{-1}$ for the Medes cell (Fig. 8b).

According to Figure SI-4(b), Banyuls is the downwelling

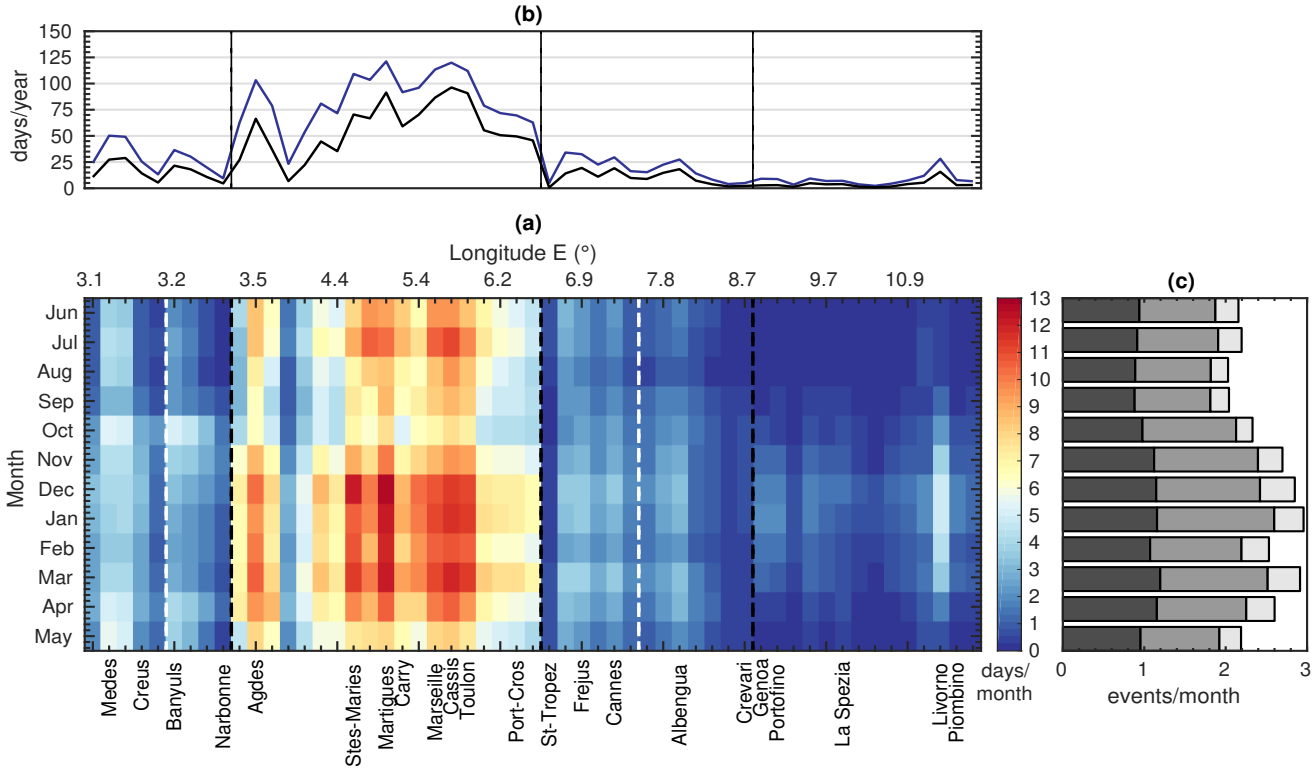

Figure 8: Spatio-temporal variability of wind-driven upwelling along the North-West Mediterranean coastline as deduced from a monthly climatological events database constructed over 1979-2019. (a) Hovmöller diagram (non-linearly spaced longitude vs time) of the mean number of wind-driven upwelling days per month for each of the 55 potential cells. The black vertical dotted lines highlight different sub-regions, the white vertical dotted lines symbolize the French borders. (b) Mean number of wind-driven upwelling days per year for the 25 % statistically-derived thresholds (blue line) and for *extreme events* (black line, equivalent to the 5% most intense wind sequences). (c) Mean number of upwelling events per cell and per month over the study area as a function of their durations : < 18 hours (dark gray), 18 hours-2 days (medium gray), > 2 days (light gray).

cell for which the maximal onshore transport (of -4×10^7 m^3 per meter of coastline) is obtained during February and December. The white crosses for the Medes cell during winter and for the Banyuls cell in February suggest that the "event analysis" (Fig. 9) slightly underestimates the impacts of wind forcing due to the thresholding procedure.

E-GoL : Agde to Port-Cros

This region is the most intense upwelling zone of the studied coastline, with 5-13 d.mo^{-1} of upwelling-favorable winds with 4 local maxima: one situated between Beziers and Montpellier (peaking at the Agde cell), one located off the Camargue region (peaking at the Saintes-Maries-de-la-Mer cell), one on the Côte Bleue (peaking at the Martigues cell) and one from the Calanques to Toulon (peaking at the Cassis cell). Those cells display strong upwelling occurrence, with values exceeding 100 d.y^{-1}, while the mean occurrence for the section is about 80 d.y^{-1}.The coast from Toulon to St-Tropez is also characterized by moderate upwelling favorable wind conditions reaching 5-8 d.mo^{-1}.

This section also presents downwelling favorable wind conditions from October to April (3-7 d.mo^{-1}), with a maximum of 7 d.mo^{-1} at Cassis in October, and a mean of downwelling favorable conditions of 30 d.y^{-1}.

On Figure SI-4(a) Cassis and Toulon cells exhibit the highest offshore water transport, with values of 3-4×10^7 m^3 per meter of coastline, from December to January. Apart from those two cells where the "event analysis" may underestimate the actual intensity of extreme events, the rest of the cells tend to be evaluated similarly by both methods.

W-Lig : St-Tropez to Crevari

This coastal zone is characterized by relatively low occurrences (25 d.y^{-1}) of both upwelling and downwelling favorable forcings (Fig. 8b and 9b). There are up to 5 d.mo^{-1} of upwelling favorable wind around Frejus, Cannes and Albengua more or less all year long. For downwelling, there are around 2-9 d.mo^{-1} of downwelling favorable wind especially from late autumn to early spring. The maximum occurrence frequency of 9 d.mo^{-1} is obtained near the Albengua coast in Italy where a small downwelling cell is active during winter months.

E-Lig : Genoa to Piombino

This section is characterized by very rare favorable wind forcing, with a mean of 20 d.y^{-1} of both upwelling and downwelling events (see Fig. 8b and 9b). A noticeable maxima reaching 5 d.mo^{-1} of downwelling and 6 d.mo^{-1} of up-

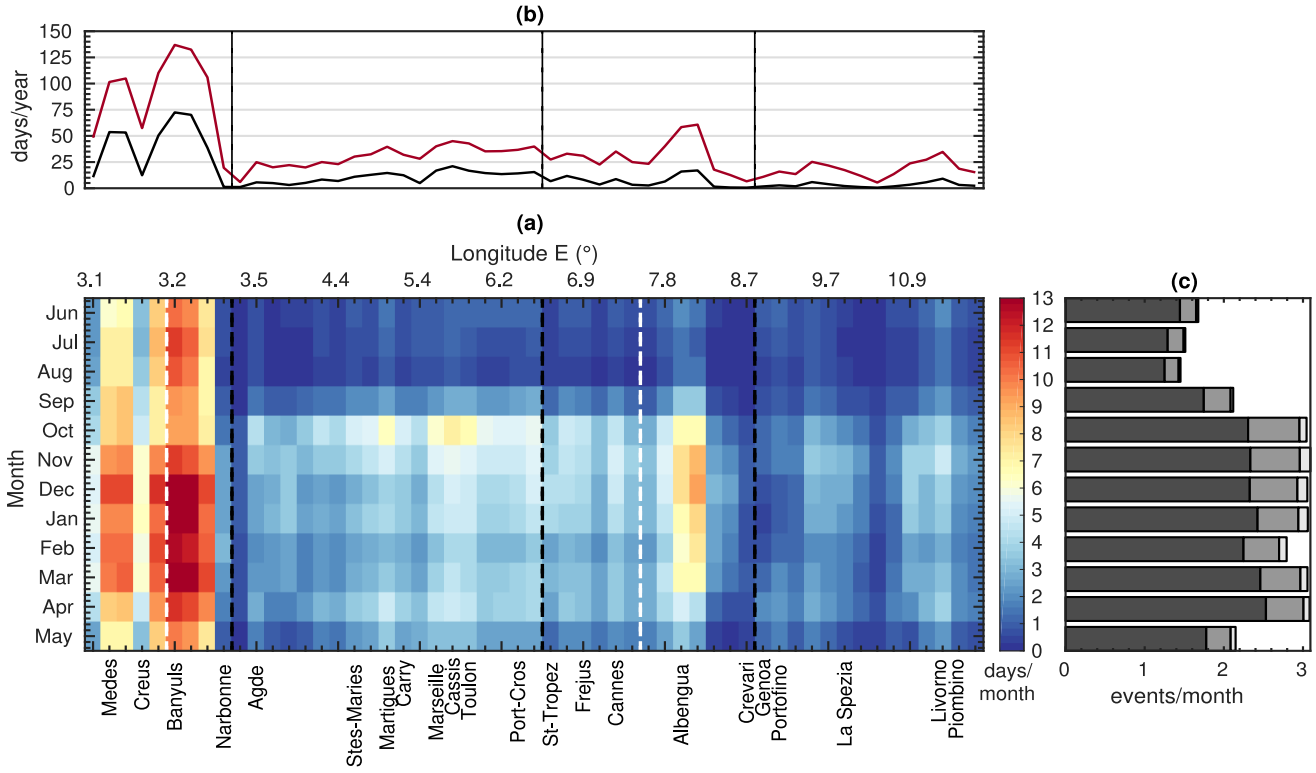

Figure 9: Spatio-temporal variability of wind-driven downwelling along the North-West Mediterranean coastline as deduced from a monthly climatological events database constructed over 1979-2019.(a) Hovmöller diagram as in Fig. 8 but for downwelling event. (b) Same as Fig. 8 but for downwelling events. (c) Same as Fig. 8 but for downwelling events.

welling are found for a small cell activated during winter months around Livorno, as also confirmed by the climatology of Ekman transport (Fig. SI-6).

4. Discussion

4.1. Upwelling and Downwelling Events on the North-Western Mediterranean coastlines

Using 40 years of high-resolution gridded Sea Surface Winds from ERA5 reanalysis, we conducted a systematic analysis of wind-forced up/downwelling events along the Northwestern Mediterranean coastlines at 20 km spatial horizontal resolution. Focusing on the most intensely forced events (top 25%), that are statistically associated to significant thermal responses according to the stratification, our analysis allows building a robust event database based on statistically-defined thresholds of alongshore wind speeds. The values of the retained thresholds (5.15 $m.s^{-1}$ for downwellings and 5.84 $m.s^{-1}$ for upwellings) are consistent with the alongshore wind forcing upwelling thresholds of 5 $m.s^{-1}$ of García-Reyes et al. (2014) and -8.5 $m.s^{-1}$, in the southern hemisphere, of Rossi et al. (2014). Due to the high statistical power (i.e. robust to small changes of statistics, such as a few more or less years/sites) and the fact that our values compare well with other published estimates, we expect that the statistical thresholds allowing the selection of the most significant events are rather conservative and should be valid for other coastal regions. Note that these threshold are theoretically a function of the statistics considered; consequently, studying the long-term trends of these wind-forced processes would require accessing a few extra decades of observations (not yet available unfortunately). Nevertheless, the climatogical analysis concerning 1979-2019 highlights clear spatial zonation and temporal variability in the occurrence, intensity and duration of sporadic wind-induced up/downwelling events.

Overall, two main areas prone to frequent downwelling and upwelling events (up to 13 $d.mo^{-1}$) were identified: the W-GoL and E-GoL areas, as previously suggested (Bakun and Agostini 2001). In addition, our study highlights specific seasonality: the E-GoL upwelling cells light up more frequently, with more intensity and longer events during wintertime. This is aligned with the wind-based approach of Bakun and Agostini (2001) who found higher upward vertical velocities due to stronger wind forcing in winter. We also find higher occurrence of downwelling events with stronger intensity on the Medes-Narbonne coastline in winter. This is consistent with the more frequent occurrences of Mistral and Tramontane events in winter (Jacq et al. 2005). Finally, in contradiction with Bakun and Agostini (2001) who reported increased vertical velocities during summer in the Ligurian sea, our results show instead a higher occurrence of upwelling events there during autumn-winter than summer, in agreement with Casella et al. (2011). For the E-GoL, we identify several upwelling cells located off Agde (namely, Sètes and Valras), along the Camargue coast (Saintes-Maries-de-la-Mer), off Côte Bleue (Méjean, Carry-Le-Rouet) and

around the Calanques region (Marseille-Riou, Cassis), in agreement with earlier study (Millot 1979). For example for the Cassis cell in July (Figure 8a), the mean 11 d.mo^{-1} of upwelling favorable wind is predicted to produce in average 11 days of upwelling per month characterized by a mean surface temperature drop of -4.4°C (see Table 4). This is in agreement with the high occurrence frequency (30%) of upwelling events in this zone during summer, evidenced from *in-situ* observations solely (Bensoussan et al. 2010). In winter the maximum 13 d.mo^{-1} of upwelling favorable wind is expected to generate in average 13 days of upwelling per month characterized by a mean surface temperature drop of -0.6°C (Tab. 4).

The wind forcing these upwellings is the Mistral, which tends to blow from North to South in the Rhône valley to then veer gradually westward (see Fig. 1) when blowing above the sea without any topographic constraints (Jacq et al. 2005). As it follows the French coastlines towards the Ligurian sea, the intensity of the Mistral tend to decreases. Nevertheless, , the intense Mistral episodes that extend far to the East are shown here to activate upwelling cells associated with zonally oriented coastal segments along the most eastern parts of the E-Gol region and along the first half of W-Lig. Our results indeed show the existence of previously overlooked upwelling cells in this region despite high (120 d.y^{-1} off Cap Sicié/Toulon) to moderate (75 d.y^{-1} from Toulon to St-Tropez) occurrences. Upwelling SST signals at Toulon were already identified by Millot and Wald (1980) but they were attributed to the advection of a cold-water plume upwelled further west. Conversely, by considering each segment of coastline individually, we show here that Toulon is prone to the sporadic activation of an upwelling cell there. Additional newly identified upwelling cells located in W-Lig include portion of coastlines around Fréjus and Cannes (25-35 d.y^{-1}) as well as off Albengua (25 d.y^{-1}). This is consistent with a previous study that simulated coastal upwelling forced by exceptional Mistral events along this Ligurian coastline (Small et al. 2012). Our results also suggest the existence of rare and short-lived upwelling events further East, for example off Levanto and Livorno (see also the spatially-confined blue shading exemplifying cold-water resurgence there during the July-2012 upwelling event presented in Fig. 1), appearing mostly during wintertime when the strongest Mistral storms occur (Jacq et al. 2005). Interestingly, we also found a significant occurrence of seasonal downwelling events in regions known for upwelling favorable winds. They mainly occur from autumn to spring since they are forced by sporadic but very intense south-eastern storms (Millot 1990).

Concerning downwelling, the most conspicuous area lies from Medes till South of Narbonne (Fig. 9) and is in good agreement with the prominent downward velocities located in the southwestern GoL (Bakun and Agostini 2001). Downwelling events occur up to 130 d.y^{-1}, that is when strong Mistral and/or Tramontane wind (oscillating between west to north-northwest direction) blow in this region (Jacq et al. 2005). Two other noticeable downwelling cells identified by our approach are around Albengua with more than 50 d.y^{-1} mainly during winter. The Albengua downwelling cells are the result of strong easterlies, which are typical storm-like weather patterns occurring in late fall/winter while being usually associated with rainy episodes.

With our statistical approach we demonstrate that wind-driven sporadic up/downwelling events occur up to 13 d.m^{-1} for the most active months (winter), and up to 125 d.y^{-1} for the most active regions, with significant cooling/warming of the coastal ocean. Although less important than the permanent Eastern Boundary Upwelling Systems, occurrence frequency of sporadic upwelling events in the E-GoL is far from being negligible for this relatively oligotrophic region. For instance, the 120 d.y^{-1} occurrence at Cassis and Toulon cells is lower but close to the maximum annual occurrence of 210 d.y^{-1} for the Iberian Peninsula upwelling (Alvarez et al. 2011). As such, sporadic wind-driven events could be seen as the primary driver of the high-frequency variability of the coastal ocean with implications not only for the temperatures but also likely for nutrient fluxes (Jacox et al. 2018), biogeochemistry and plankton communities (Armbrecht et al. 2014).

Moreover, the frequency of occurrence of up/downwelling events along North-West Mediterranean coastlines is comparable to other intermittent coastal systems. Off southeast Australia, Rossi et al. (2014) found a mean of 3-10 d.mo^{-1} of upwelling-favorable wind forcing during summer and an annual mean of 15-55 d.y^{-1}. The most active cells identified in the E-GoL have more frequent upwelling favorable wind (more than 100 d.y^{-1}) than the ones located off southeast Australia. In this mostly downwelling-favorable area, Rossi et al. (2014) found an annual mean of downwelling favorable wind forcing of 60-120 d.y^{-1}, which is comparable to the mean of ∼80 d.y^{-1} found in the W-GoL.

With this approach we have shown that in the North-West Mediterranean Sea significant wind-driven sporadic up/downwelling occur regularly (up to 13 d.m^{-1} for the most active months, and up to 125 d.y^{-1} for the most active regions) and are more frequent and intense in winter.

4.2. Ocean Response Coupled to Wind-Forced Events

Coastal processes induced by alongshore winds can exert a strong influence on the physical and biogeochemical characteristics of the coastal ocean (Mackas et al. 2006; Rossi et al. 2014). We characterize the thermal responses of the coastal ocean through the joint statistical analyses of alongshore winds (upwelling and downwelling forcings) and *in-situ* near surface (10 m) and subsurface (35 m) high-frequency temperature variations recorded over multiple years at 11 coastal sites. We find two levels of thermal response linked to the seasonal regimes of open-ocean stratification (D'Ortenzio et al. 2005). Note however that the precise separation between stratified versus unstratified conditions varies locally (Tab. 3 and Fig. SI-2 to SI-5).

During wintertime, the top 50-m of the coastal water column tend to be well-mixed and may reach down to ∼13-14°C

(Fig. 4b), likely due to enhanced air-sea fluxes and wind-induced vertical mixing. In addition to the offshore convection events occurring each year during winter, the temperature drops over shallow areas like the GoL can be stronger (down to 10°C), all of this leading to the sinking and cascading of colder and denser waters and the creation of intermediate or deep water masses (Madron et al. 2013; Houpert et al. 2015; Houpert et al. 2016). Despite the super-imposition of this large-scale process, we are still able to detect relative cooling (of low intensity) after wind-driven upwelling events despite the lack of coastal stratification in winter. Note that downwelling favorable wind could also be responsible for local vertical mixing (for example the wind event from 23-Feb-2013 to 26-Feb-2013 in Fig. 6). This particular event could also be due to the horizontal transport of cold water upwelled in the eastern GoL toward the Catalan shelf, hence overcoming the local warming signal expected from the downwelling favourable wind (Mikolajczak et al. 2020).

Our statistical approach evidences that upwelling events (WUDI>0) are associated with 10m surface layers cooling (2nd column of Tab. 3) and downwelling events (WUDI<0) are associated with 35m layer warming (last column of Tab. 3) for all sites, while the amplitude of the temperature variation under unstratified condition is lower than during stratified periods.

Overall, our results reveal frequent, intense and short-lived coastal cooling events at the main E-GoL upwelling cells and coastal warming events of similar characteristics in the case of W-GoL downwelling cells. The temperature response intensity allows a first ranking of the potential incidence of these processes in terms of hydrographic conditions. At Carry-le-Rouet, Méjean, Marseille-Riou, Cassis and Toulon cells, upwelling events are not only more frequent than elsewhere, but they also translate into significantly more intense cooling than any other upwelling cells (e.g. for the most extreme sequence, median responses are -4.98°C for Toulon and -5.63°C for Méjean, as compared to -2.0°C for Port-Cros and -2.9°C for Agde (Tab. 3).

Concerning downwelling, Banyuls and Cassis have comparable thermal responses to extreme downwelling favorable wind forcing : +1.75°C per event for Cassis versus +2.38°C for Banyuls under stratified conditions (Tab. 3). Nevertheless, Banyuls is described as a prominent downwelling cell because of the more frequent occurrence of favorable wind-forcing (10 days in September in comparison to only 2 days for Cassis, Fig. 9a). For upwelling, note that cells experiencing similar forcing statistics, such as Agde and Carry-Le-Rouet cells in July (approximately 10 $d.mo^{-1}$, Fig. 8a), may display surface cooling of different intensity: the median response of an event for Carry-Le-Rouet is -5.08°C as compared to -2.9°C for Agde (Tab. 3). Although further analyses are required to understand these discrepancies, the larger continental shelf off Agde could explain why upwelled waters are sourced to shallower depths, hence being relatively warmer than those upwelled over the narrower shelf off Carry-Le-Rouet (Estrade et al. 2008; Rossi et al. 2013).

Using our events database we were also able to estimate the Ekman transport, which integrates wind-forcing intensity over the event duration, thus reflecting the overall magnitude of both processes, in good agreement with our wind-forcing favourable event analysis. According to Figure SI-4b, Banyuls and Medes are the cells of highest predicted onshore Ekman transport, confirming the most intense coastal convergence processes associated with downwelling events. According to Figure SI-4a, and complementing previous findings from Millot (1979), Toulon and Cassis are the coastal cells with highest predicted offshore Ekman transport, highlighting them as the most intense of all northwestern Mediterranean upwelling cells.

The small differences between our event-based and Ekman transport analyses, along with the variable thermal responses among sites and events, confirm that there are other physical processes and factors that are affecting the thermal responses of the coastal ocean. Those factors include (i) the local bathymetry (shelf width and slope inclination) modulating the uplift of cold deep waters; for instance, submarine canyons such as the ones off Cassis have been suggested to favour cold-water resurgence there (Alberola and Millot 2003) (ii) internal waves (Puig et al. 2001) and (iii) traveling eddies or fronts influencing temperature directly and/or the advection of upwelled waters (Taupier-Letage et al. 2003; Casella et al. 2011; Rossi et al. 2013; Mikolajczak et al. 2020). So, even if we consider events generated by similar wind-forcing, these neglected factors could easily explain the difference in median temperature responses and delays between sites (Tab. 2 and 3) as well as the dispersion in Fig. 7. More specifically, an example of a local physical process affecting the high frequency variability of water temperature is the mesoscale anticyclonic eddy often appearing off the Roussillon coast. This eddy could influence ocean temperature response to atmospheric forcing for Cape Creus, Medes and Banyuls cells (Kersalé et al. 2013). Other sources of ocean temperature variation in the Mediterranean Sea are intrusions of the Northern Current that can flush the E-GoL area within 2–3 days (Ross et al. 2016; Barrier et al. 2016) and exceptional freshwater discharges (e.g. Rhône river plume) for the nearby cells along the downstream Camargue coast or the upstream Côte Bleue (Méjean, Carry-Le-Rouet) when the plume extends eastward (Fraysse et al. 2014).

An additional factor influencing the temperature response is the recent thermal history of the surrounding waters. If shortly after a first upwelling, another favorable wind forcing occurs, it will trigger a quicker and stronger coastal cooling, meaning that the temporal succession of wind events has an influence on the delay and intensity of the response (Benazzouz et al. 2014). An example of that can be found in Fig. 3b where, of the two events starting on 09/09/2013 and 16/09/2013, the maximal negative temperature anomaly was attained more quickly for the second one. This "temporal memory" could be the reason why the temporal lags reported in Tab. 2 are quite variable. Nevertheless, because those lags are obtained using multi-annual time-series (i.e. statistically sampling all type of events' successions), we expect

that they give meaningful estimates of the mean temporal lag between wind forcing and ocean temperature response. Moreover, the range of lags found for wind-forced upwelling events in the Gulf of Lion (6-36h, excluding Agde, see Tab. 2) is consistent with Millot (1990) who reported the apparition of cool upwelled water on SST satellite images about one day after the onset of strong Mistral. Lags for the sites between Méjean and Portofino, Toulon excepted, are also in agreement with the 2-d lag found by Rossi et al. (2014) for sporadic upwelling off southeast Australia.

It is worth noting that there could be a spatial mismatch between the real location of the upwelling cell and the actual record of seawater temperature, thus affecting the temporal delay. In other words, recently upwelled cold waters from an active nearby upwelling cell could take some time to reach the closest downstream temperature sensors. This may explain the longer lags (54-66h) reported at Agde. In this respect, the thermo-loggers located within semi-enclosed marinas or artificial coves (Rey et al. 2020) may not be the best proxies of intermittent wind-driven events as some may miss or underestimate the thermal responses that are best captured in the close vicinity of active cells. This also means that if up/downwelling cells are effectively co-located with the temperature monitoring location, then they should return high correlation and short lags. Under these considerations, another way to interpret the statistical lags (Tab. 2) could allow estimating how far is the actual cell from the monitored site. For example, Cassis and Toulon sites are likely to be located near an active cell for both upwelling and downwelling, while Banyuls sites would be located near a downwelling cell, which is also confirmed by the statistical events analysis (Fig. 8 and 9).

4.3. Uncertainties Linked to the Methodological Choices and Neglected Processes

Even if the validity of Ekman's assumptions is uncertain for our atmospheric forcing and area of study (see next sect. 4.4), WUDI is well correlated with water temperature variations (see Fig. 3, 4, 5, 6, and Tab. 2 to 4). While interpretating this index as the ideal indicator of the "true" cross-shore water transport is questionable, we use it here as a generic tool to define and quantify favorable wind forcing events, allowing us to build a climatology of upwelling and downwelling events in our area of study.

Regarding the atmospheric forcing, the ERA5 SSW product tends to underestimate high wind speeds in the NW Mediterranean Sea wind speeds (Vannucchi et al. 2021). This suggest that our approach is conservative, e.g. more numerous and stronger wind-driven events would be captured if *in-situ* winds were available for each coastal cell. Moreover, ERA5, that we chose mainly for its 40 years time coverage, has a relatively large grid cell modelling. Our wind-based index would gain in precision by using higher-resolution SSW taking into account local orography, such as AROME (Müller et al. 2017) or WRF (Powers et al. 2017) models that could be used to forecast upwelling or downwelling events.

The discretization of the coastline has an important impact in the results obtained too. Since the scale considered was 20 km, some coastlines with complex patterns, like Capes and Gulfs may not have been resolved perfectly, despite its proven influence on coastal upwelling signatures (Crepon and Richez 1982; Crepon et al. 1984). An example could be the Gulf of Fos (near Martigues cell in Fig. 8, 9 and SI-6): the shoreline angle attributed to this cell could introduce a bias and result in higher upwelling occurrence there as compared to Marseille-Riou and Cassis, while its main general orientation seems not as favorable as the Calanques coastline for upwelling. Another example is Cape Creus (W-GoL), which might provide different results with a smaller discretization scale.

The general approach to build Fig. 7 consisted in using all the available *in-situ* temperature time-series to obtain statistical estimates of the ocean response to wind forcing that are then considered valid for the whole North-West Mediterranean coastlines. Better estimates could be obtained if oceanic temperatures were monitored in many more coastal sites in our studied area. Note indeed that some monitoring sites are not favorable to up/downwelling events and/or are located far away from the upwelling source points. Consequently, considering an higher number of well-placed monitoring sites with longer temporal coverage would undoubtedly increase our correlations and sharpen our evaluation of the wind-forcing/temperature relationships. The methodological choice of merging event separated by 1 day or less, as in Millot (1979), for the definition of our events has a small impact on the final result. A shorter merging time would return more numerous, but shorter and less intense, events. A longer merging time would result capturing less events but overall with longer duration and higher intensity. The different choices for this merging time could affect the values in Figures 8, 9 and SI-6, but would not affect the general pattern nor our general conclusions. Moreover, the results of the lagged-correlation approach in Table 2 validate the order of magnitude of this merging time, as the lags found vary between 0.25 and 2.25 days with a predominance of 1 to 1.5 days for the sites with the highest correlations.

The WUDI thresholds selected for the event detection have an impact mainly on the duration of the events retained. These thresholds considered the top 25% most intense wind forcing episodes because the objective was to retain a category of strong events that have significant ocean temperature responses. Another threshold defining even stronger events, based on the 5% most intense sequences, was tested to define "extreme" events, those events display similar patterns but lower occurrences (Fig. 8b and 9b). As discussed previously, those values of alongshore wind intensity are conservative and coherent with other upwelling studies.

In this work we focus on the most significant upwelling (downwelling, resp.) events resulting from transient wind-driven coastal divergence (convergence, resp.) while neglecting the process referred to as Ekman pumping (i.e. wind curl, evaluating the spatial variation in the wind field). While Schaeffer et al. (2011) showed the determining influence of wind stress curl to represent both a mesoscale eddy and a

specific upwelling cell in the northwestern GoL, we believe it can be reasonably disregarded here since the spatio-temporal scales over which it primarily acts are larger than the 20-km cells and daily time-scales considered here.

Note also that our approach does not take into account the drag effect of the cross-shore wind for such transient wind, despite potentially explaining some of the time lags observed between Ekman transport and the actual wind forcing. The geostrophic limitation imposed by the Northern Current was also neglected in our study despite its potential to may substantially alter the vertical transport originating from wind-based estimates (Marchesiello and Estrade 2010; Rossi et al. 2013). More specifically, it would dampen upwelling and favor downwelling for the cells most exposed to the cross-shore pressure gradient, such as in both E-Lig and W-Lig regions (i.e. where the current is well defined and most intensely flowing close to the coast). The different statistics reported for Toulon and Port-Cros cells are perhaps due to this effect: while Port-Cros sees roughly 1/3 less upwelling favourable winds than Toulon, the mean thermal response at Port-Cros exhibits less than half of the magnitude recorded at Toulon and has much lower correlation with WUDI. The wind-driven cooling at Port-Cros may be often diminished due to the Northern Current warm waters that overcome and/or push westward the upwelled cold waters during and after an event, leading to faster relaxation. To better understand how the geostrophic limitation modulates wind-forced processes, a multi-sensor analysis combining data from the pressure-sensors scattered along the coast (Rey et al. 2020) and satellite altimetry could help assessing the spatial variability of the cross-shore pressure gradient.

4.4. Theoretical Assumptions and Index Formulation

Despite the fact that Ekman theory has been widely used to produce various upwelling indices across a range of coastal oceanic systems using different wind products and different methods, we now revise the index formulation and the neglected processes. Similarly to other modified Bakun index, WUDI is based on Ekman's theory that assumed a steady, homogeneous, horizontal flow with friction on a rotating earth (Stewart 2008). The validity of these simplifications, in particular of the "deep-water", "steady-state" and "vertical viscosity" assumptions, need to be discussed.

The "steady-state" assumption is strictly valid only if, for the event considered, the forcing wind blows for a time period longer than a pendulum day, which is approximately 17 hours at our latitudes. In our event database, more than half of all events last more than 18 hours. Note however that the event duration is computed as a time period during which alongshore wind exceeds our conservative thresholds (Tab. 4), meaning that the wind start blowing before and continue to be favourable after the event delimitations (see also Fig. 2 and its caption). In other words, the durations reported in Fig. 8c and 9c are largely underestimating the actual duration of favourable wind forcing. Another evaluation can be achieved by re-interpreting the statistical approach used to establish the WUDI thresholds (sect. 3.2.2). Among the 25% most significant wind forcing sequences (i.e. time period with WUDI>0 or WUDI<0, see sect. 2.4.2), 86% of upwelling WUDI sequences and 74% of downwelling WUDI sequences last longer than 2 days. This shows that for a large majority of events considered here, the up/downwelling favorable winds blow during far longer than a pendulum day, making the steady-state assumption valid. For the remaining minority of events, the assumption could be false, suggesting that the computed Ekman transport could have been marginally overestimated for these non-representative events.

Concerning the "deep-water" assumptions, it appears valid for the majority of the studied cells that stand nearby deep areas (>> 200 m, see the isobaths in Fig. 1). This is because they are located over narrow continental shelves, in the immediate vicinity of steep slopes reaching depths of several thousand meters. For these "deep" cells, the surface Ekman layer would fully develop while the cross-shore wind-driven circulation would be minimally affected by bottom friction, providing high confidence in WUDI predictions there. Some exceptions are the coastal cells located over extended continental shelves (south of Portofino in E-Lig and Banyuls and Agde in the western GoL) that appear surrounded by areas less deep than 200 m. For these "shallow" cells, the bathymetry can lead to the merging of both surface and bottom Ekman layers that could interrupt Ekman transport and induce an offshore displacement of the main upwelling cell (Estrade et al. 2008). Another consequence is the slowdown of the cross-shore circulation due to enhanced bottom friction, potentially diminishing Ekman transport divergence (Lentz 2001; Estrade et al. 2008). While the former effect seems not relevant here (to our knowledge, there is no evidence of mid-shelf or shelf-break upwelling signatures in these regions), the latter process would suggest that WUDI predictions tend to overestimate horizontal water transport and the response magnitude.

Last but not least, both Ekman theory and WUDI assume a constant vertical eddy diffusivity A_z. Although horizontal Ekman currents depend theoretically on the vertical viscosit ymagnitude and structure, the vertically-integrated Ekman transport (used in the WUDI calculation) does not depend on the vertical viscosity. Nonetheless, in nature, vertical viscosity is driven by turbulent processes and varies in space and time. Vertical eddy diffusivity tightly relates to stratification, which is also controlled by momentum (wind forcing) and heat fluxes at the ocean surface. This means that WUDI ignores the true stratification. Analysing the ocean thermal responses separately into two regimes, namely stratified and unstratified, is a somehow simplistic approach to take this limitation into account. However, since autumn and spring are transitional periods between deep thermoclines and shallow but strong near-surface stratification (Fig. SI-2-5), future research could aim at developing indices that readily consider the variability of A_z and/or of the stratification through d_E (Ashkenazy et al. 2015). Indeed, it also means that WUDI disregards how the actual SML relates with the Ekman depth d_E. To have a better understanding of how they

compare, back-of-the-envelope computations allow estimating the typical range d_E in our region. Following Stewart (2008), we have

$$d_E = \sqrt{\frac{2\pi^2 A_z}{f}} \tag{3}$$

And

$$d_E = \|W\| * \frac{7.6}{\sqrt{\sin(\phi)}} \tag{4}$$

By modifying Eq. 1 to take into account C_d, and for the latitudes considered (42°N-45°N), with wind speeds varying between 5 m.s^{-1} and 25 m.s^{-1}, Eq. 4 returns that d_E spans approximately 20-170 m. It matches well the typical surface mixed-layers observed throughout the year in the region (D'Ortenzio et al. 2005) while it has substantial variations. Overall, when the SML is deeper than the Ekman depth (e.g. mostly during winter), the Ekman transport estimated by WUDI could be less than the actual one involving thicker SMLs. However the vertical thermal gradient is expected to be small, leading to low temperature anomalies, as reported in Fig. 7. If the SML is shallower than the Ekman depth, WUDI would overestimate the associated Ekman transport, despite potential compensation by the large thermal responses typical of stratified periods. This would particularly affect the events occurrence during summer, when SMLs may be thinner than 50 m (D'Ortenzio et al. 2005). In this case, the mixing conditions change rapidly and variable estimates of the vertical viscosity could improve the reliability of WUDI. Note that by using Eq. 3 and previous d_E estimates, the range of vertical eddy diffusivities is $A_z \in [2 \times 10^{-3}; 2 \times 10^{-1}]$ ($m^2.s^{-1}$), which corresponds to average vertical mixing conditions consistent with the literature Herrmann et al. (2008). How local or long-term changes in stratification affect each coastal upwelling cell and its oceanic response is a complex topic falling beyond the scope of this study.

Even more complex is how wind, stratification and topography interact together to control the lag and the intensity of the coastal ocean responses to wind-forced events. One option could be to develop analytically, and test against observations, an improved index formulation that considers simultaneously SSW fine-scale patterns and the local shelf topography along with variable stratification, geostrophic limitation, wind stress curl. Another research direction could use numerical models to test all factors and situations independently in order to improve our ability to understand such intermittent events and predict their impacts in the coastal ocean. Nonetheless, the widespread and successful applications of our simplified index (Bakun 1975; Alvarez et al. 2011; Rossi et al. 2014; Jacox et al. 2018), the fact that WUDI correlates well with observed temperature anomalies and the large statistics employed here give high confidence in the main results highlighted here.

5. Conclusion

In this study we developed a wind-based up/downwelling index (WUDI) computed from gridded SSW reanalysis data that we validated and calibrated with *in-situ* temperature observations along North-West Mediterranean coastlines. We analyzed statistically the ocean temperature changes due to strong wind events allowing us to define thresholds, that are then used to build a database of up /downwelling events over the last 4 decades. Each of these events can be associated to a median thermal response depending on the stratification regime. Moreover, a mean delay of this temperature response was found to be ∼27 hours for upwelling events and ∼32 hours for downwelling events, although it varies from-site-to-site probably due to local factors. A seasonal climatology of events showed that up to 13 days per month of upwelling occur along the coast from Camargue to Toulon, while downwelling events prevail from Medes to Banyuls, with a maximum of 13 days per month at Banyuls. The most intense up/downwelling favorable wind forcing occur during winter months (December to March) and are associated with weaker, yet measurable and quantified statistically, thermal responses than during summer events. Finally, we confirmed the existence of previously identified up/downwelling cells and we demonstrate the existence of new small cells active for upwelling and/or downwelling, like the ones in Frejus, Albengua or Livorno. Those small cells appear principally during winter and are 2 to 4 times less active than the major ones.

With this multi-sensor approach of sporadic up /downwelling we identified the spatial and seasonal occurrence of up /downwelling favorable wind forcing, and we were able to link the intensity of the temperature response to its respective favorable wind forcing along the North-Western Mediterranean coast. The multi-decadal WUDI dataset provided here could be useful to evaluate the skills of regional hydrodynamical models. Moreover, WUDI could be helpful to guide future studies, to interpret satellite data as well as to examine ocean/atmosphere interactions in the coastal ocean. Here we studied the periods and locations of active up/downwelling cells and their local effects, which can be of interest for coastal spatial planning. Future studies could investigate the spatial extension and transport pathways of upwelled waters, as well as their chemical and biological impacts. Finally, similar analyses could investigate the long-term occurrences and Mediterranean-scale impacts of such intermittent wind-forced coastal processes.

Data's availability statement

Upon acceptation, we will make publicly available the WUDI time-series for each of the 55 coastal cells, along with a read-me file, at this repository. Concerning raw temperature data, they can be officially requested online through the T-MEDNet network; a data paper is currently in preparation. ERA5 raw SSW data can be downloaded through the Climate Data Store managed by Copernicus.

Declaration of competing interest

Acknowledgments

R.O., N.B., C.P. and V.R. acknowledge financial support from the European Commission through the programme "Caroline Herschel" (FPACUP_SGA4_Tier1; agreement number: 2020/SI2.833213) through the project entitled "Developing Downstream applications and services on BIO-PHYsical characterization of the seascape for COASTal management" (BIOPHYCOAST). The authors thank the coordinators and members of the T-MEDNet network for providing their observation data, and particularly : Joaquim Garrabou (Institut de Ciències del Mar), Victoria Riera (Parc Natural Cap de Creus), Ronan Rivoal (Réserve Naturelle Marine de Cerbère Banyuls), Sylvain Blouet (Aire Marine Protégée de la côte Agathoise), Eric Charbonnel (Parc Marin Côte Bleue), Dorian Guillemain (OSU Institut Pytheas), Stephane Sartoretto (IFREMER), Marion Peirache (Parc National Port-Cros) and Valentina Cappanera (Portofino Marine Protected Area). The SST map presented in Figure 1 originates from the OSIS database (MIO-SATMOS ; PI. I. Taupier-Letage). The authors thank two anonymous reviewers and the editor for their constructive comments that helped improve the original manuscript.

References

Alberola, C and Claude Millot (Apr. 2003). "Circulation in the French mediterranean coastal zone near Marseilles: The influence of wind and the Northern Current". In: *Continental Shelf Research* 23, pp. 587–610. DOI: 10.1016/S0278-4343(03)00002-5.

Alberola, C, S Rousseau, Claude Millot, M Astraldi, J Font, J Garcialafuente, Gp Gasparini, U Send, and Annick Vangriesheim (1995). "Tidal currents in the western mediterranean-sea". In: *Oceanologica Acta* 18.2. Ed. by Gauthier-Villars, pp. 273–284.

Alvarez, I., M. Gomez-Gesteira, M. deCastro, M.N. Lorenzo, A.J.C. Crespo, and J.M. Dias (Apr. 2011). "Comparative analysis of upwelling influence between the western and northern coast of the Iberian Peninsula". In: *Continental Shelf Research* 31.5, pp. 388–399. ISSN: 02784343. DOI: 10.1016/j.csr.2010.07.009.

André, Gaël, Pierre Garreau, Valérie Garnier, and Philippe Fraunié (Dec. 2005). "Modelled variability of the sea surface circulation in the Northwestern Mediterranean Sea and in the Gulf of Lions". In: *Ocean Dynamics* 55.3, pp. 294–308. ISSN: 1616-7341, 1616-7228. DOI: 10.1007/s10236-005-0013-6.

Armbrecht, L. H., M. Roughan, V. Rossi, A. Schaeffer, P. L. Davies, A. M. Waite, and L. K. Armand (Mar. 2014). "Phytoplankton composition under contrasting oceanographic conditions: Upwelling and downwelling (Eastern Australia)". In: *Continental Shelf Research* 75, pp. 54–67. DOI: 10.1016/j.csr.2013.11.024.

Ashkenazy, Yosef, Hezi Gildor, and Golan Bel (Aug. 2015). "The effect of stochastic wind on the infinite depth Ekman layer model". In: *EPL (Europhysics Letters)* 111.3, p. 39001. DOI: 10.1209/0295-5075/111/39001.

Bakun, Andrew (1973). *Coastal Upwelling Indices, West Coast of North America, 1946-71*, p. 112.

— (1975). *Daily and Weekly Upwelling Indices, West Coast of North America*. United States: NOAA Tech. Rep., p. 124.

Bakun, Andrew and Vera Natalie Agostini (Sept. 30, 2001). "Seasonal patterns of wind-induced upwelling/downwelling in the Mediterranean Sea". In: *Scientia Marina* 65.3, pp. 243–257. ISSN: 1886-8134, 0214-8358. DOI: 10.3989/scimar.2001.65n3243.

Barrier, Nicolas, Anne A. Petrenko, and Yann Ourmières (Mar. 2016). "Strong intrusions of the Northern Mediterranean Current on the eastern Gulf of Lion: insights from in-situ observations and high resolution numerical modelling". In: *Ocean Dynamics* 66.3, pp. 313–327. ISSN: 1616-7341, 1616-7228. DOI: 10.1007/s10236-016-0921-7.

Benazzouz, Aïssa, Josep L. Pelegrí, Herve Demarcq, Francisco Machín, Evan Mason, Abdellatif Orbi, Jesus Peña-Izquierdo, and Mordane Soumia (Sept. 2014). "On the temporal memory of coastal upwelling off NW Africa". In: *Journal of Geophysical Research: Oceans* 119.9, pp. 6356–6380. ISSN: 21699275. DOI: 10.1002/2013JC009559.

Bensoussan, Nathaniel, Jean-Claude Romano, Jean-Georges Harmelin, and Joaquim Garrabou (Apr. 2010). "High resolution characterization of northwest Mediterranean coastal waters thermal regimes: To better understand responses of benthic communities to climate change". In: *Estuarine, Coastal and Shelf Science* 87.3, pp. 431–441. DOI: 10.1016/j.ecss.2010.01.008.

Bensoussan, Nathaniel et al. (June 30, 2019). "Using CMEMS and the Mediterranean Marine Protected Areas sentinel network to track ocean warming effects in coastal areas". In: *Journal of Operational Oceanography* 12 (sup1), S65–S73. ISSN: 1755-876X, 1755-8778. DOI: 10.1080/1755876X.2019.1633075.

Berta, Maristella et al. (July 2018). "Wind-induced variability in the Northern Current (northwestern Mediterranean Sea) as depicted by a multiplatform observing system". In: *Ocean Science* 14.4, pp. 689–710. DOI: 10.5194/os-14-689-2018.

Bourassa, Mark A. et al. (Aug. 23, 2019). "Remotely Sensed Winds and Wind Stresses for Marine Forecasting and Ocean Modeling". In: *Frontiers in Marine Science* 6, p. 443. ISSN: 2296-7745. DOI: 10.3389/fmars.2019.00443.

Bourrin, F., X. Durrieu de Madron, S. Heussner, and C. Estournel (2008). "Impact of winter dense water formation on shelf sediment erosion (evidence from the Gulf of Lions, NW Mediterranean)". In: *Continental Shelf Research* 28.15, pp. 1984–1999. DOI: 10.1016/j.csr.2008.06.006.

Casella, Elisa, Anne Molcard, and Antonello Provenzale (Oct. 2011). "Mesoscale vortices in the Ligurian Sea and their effect on coastal upwelling processes". In: *Journal of Marine Systems* 88.1, pp. 12–19. DOI: 10.1016/j.jmarsys.2011.02.019.

Chavez, Francisco P. and Monique Messié (Dec. 2009). "A comparison of Eastern Boundary Upwelling Ecosystems". In: *Progress in Oceanography* 83.1, pp. 80–96. ISSN: 00796611. DOI: 10.1016/j.pocean.2009.07.032.

Crepon, Michel and Claude Richez (Dec. 1982). "Transient Upwelling Generated by Two-Dimensional Atmospheric Forcing and Variability in the Coastline". In: *Journal of Physical Oceanography* 12.12, pp. 1437–1457. DOI: 10.1175/1520-0485(1982)012<1437:tugbtd>2.0.co;2.

Crepon, Michel, Claude Richez, and Michel Chartier (Aug. 1984). "Effects of Coastline Geometry on Upwellings". In: *Journal of Physical Oceanography* 14.8, pp. 1365–1382. DOI: 10.1175/1520-0485(1984)014<1365:eocgou>2.0.co;2.

D'Ortenzio, Fabrizio, Daniele Iudicone, Clement de Boyer Montegut, Pierre Testor, David Antoine, Salvatore Marullo, Rosalia Santoleri, and Gurvan Madec (2005). "Seasonal variability of the mixed layer depth in the Mediterranean Sea as derived from in situ profiles". In: *Geophysical Research Letters* 32.12. ISSN: 1944-8007. DOI: 10.1029/2005GL022463.

Estrade, P., P. Marchesiello, Alain Colin De Verdière, and Claude Roy (Sept. 2008). "Cross-shelf structure of coastal upwelling: A two — dimensional extension of Ekman's theory and a mechanism for inner shelf upwelling shut down". In: *Journal of Marine Research* 66.5, pp. 589–616. DOI: 10.1357/002224008787536790.

Ferrarin, Christian, Debora Bellafiore, Gianmaria Sannino, Marco Bajo, and Georg Umgiesser (Feb. 2018). "Tidal dynamics in the inter-connected Mediterranean, Marmara, Black and Azov seas". In: *Progress in Oceanography* 161, pp. 102–115. DOI: 10.1016/j.pocean.2018.02.006.

Fraysse, Marion, Ivane Pairaud, Oliver N. Ross, Vincent M. Faure, and Christel Pinazo (Oct. 2014). "Intrusion of Rhone River diluted water into the Bay of Marseille: Generation processes and impacts on ecosystem functioning". In: *Journal of Geophysical Research: Oceans* 119.10, pp. 6535–6556. DOI: 10.1002/2014jc010022.

García-Reyes, Marisol, John L. Largier, and William J. Sydeman (Jan. 2014). "Synoptic-scale upwelling indices and predictions of phyto- and zooplankton populations". In: *Progress in Oceanography* 120, pp. 177–188. ISSN: 00796611. DOI: 10.1016/j.pocean.2013.08.004.

Garrabou, Joaquim, Nathaniel Bensoussan, and Ernesto Azzurro (2019). "Monitoring Climate-related responses in Mediterranean Marine Protected Areas and beyond: FIVE STANDARD PROTOCOLS". In: in collab. with Digital.CSIC and Digital.CSIC. Publisher: CSIC - Instituto de Ciencias del Mar (ICM). DOI: 10.20350/DIGITALCSIC/8612.

Herrmann, Marine, Samuel Somot, Florence Sevault, Claude Estournel, and Michel Déqué (Mar. 2008). "Modeling the deep convection in the northwestern Mediterranean Sea using an eddy-permitting and an eddy-resolving model: Case study of winter 1986–1987". In: *Journal of Geophysical Research* 113.C4. DOI: 10.1029/2006jc003991.

Hersbach, Hans et al. (June 2020). "The ERA5 global reanalysis". In: *Quarterly Journal of the Royal Meteorological Society* 146.730, pp. 1999–2049. DOI: 10.1002/qj.3803.

Houpert, L., P. Testor, X. Durrieu de Madron, S. Somot, F. D'Ortenzio, C. Estournel, and H. Lavigne (Mar. 2015). "Seasonal cycle of the mixed layer, the seasonal thermocline and the upper-ocean heat storage rate in the Mediterranean Sea derived from observations". In: *Progress in Oceanography* 132, pp. 333–352. DOI: 10.1016/j.pocean.2014.11.004.

Houpert, L. et al. (Nov. 2016). "Observations of open-ocean deep convection in the northwestern Mediterranean Sea: Seasonal and interannual variability of mixing and deep water masses for the 2007-2013 Period". In: *Journal of Geophysical Research: Oceans* 121.11, pp. 8139–8171. DOI: 10.1002/2016jc011857.

Jacox, M. G., C. A. Edwards, Hazen E. L., and Bograd S. J. (Oct. 2018). "Coastal Upwelling Revisited: Ekman, Bakun, and Improved Upwelling Indices for the U.S. West Coast". In: *Journal of Geophysical Research: Oceans* 123.10, pp. 7332–7350. DOI: 10.1029/2018jc014187.

Jacox, M. G., A. M. Moore, C. A. Edwards, and J. Fiechter (May 16, 2014). "Spatially resolved upwelling in the California Current System and its connections to climate variability". In: *Geophysical Research Letters* 41.9, pp. 3189–3196. ISSN: 00948276. DOI: 10.1002/2014GL059589.

Jacq, Valérie, Philippe Albert, and Robert Delorme (Aug. 2005). "Le mistral, Quelques aspects des connaissances actuelles". In: *La Météorologie* 50, 30–38, link : https://www.yachter.fr/pdf/download/comprendre_le_mistral.pdf.

Johns, Bryan, Patrick Marsaleix, Claude Estournel, and Raoul Véhil (Aug. 1992). "On the wind-driven coastal upwelling in the Gulf of Lions". In: *Journal of Marine Systems* 3.4, pp. 309–320. ISSN: 09247963. DOI: 10.1016/0924-7963(92)90008-V.

Kersalé, M., A. A. Petrenko, A. M. Doglioli, I. Dekeyser, and F. Nencioli (Jan. 2013). "Physical characteristics and dynamics of the coastal Latex09 Eddy derived from in situ data and numerical modeling: STUDY OF LATEX09 EDDY IN SITU & NUMERICAL DATA". In: *Journal of Geophysical Research: Oceans* 118.1, pp. 399–409. ISSN: 21699275. DOI: 10.1029/2012JC008229.

Lentz, Steven J (2001). "The Influence of Stratification on the Wind-Driven Cross-Shelf Circulation over the North Carolina Shelf". In: *JOURNAL OF PHYSICAL OCEANOGRAPHY* 31, p. 12.

Mackas, David L, P Ted Strub, Andrew Thomas, and Vivian Montecino (2006). "Chapter 2. EASTERN OCEAN BOUNDARIES". In: 41, link : https://www.researchgate.net/publication/313194637_Eastern_ocean_boundaries_panregional_overview.

Madron, X. Durrieu de et al. (Apr. 2013). "Interaction of dense shelf water cascading and open-sea convection in the northwestern Mediterranean during winter 2012". In: *Geophysical Research Letters* 40.7, pp. 1379–1385. DOI: 10.1002/grl.50331.

Marchesiello, P. and P. Estrade (Jan. 1, 2010). "Upwelling limitation by onshore geostrophic flow". In: *Journal of Marine Research* 68.1, pp. 37–62. ISSN: 0022-2402. DOI: 10.1357/002224010793079004.

Meneghesso, Claudia et al. (Feb. 2020). "Remotely-sensed L4 SST underestimates the thermal fingerprint of coastal upwelling". In: *Remote Sensing of Environment* 237, p. 111588. DOI: 10.1016/j.rse.2019.111588.

Mikolajczak, Guillaume et al. (Dec. 2020). "Impact of storms on residence times and export of coastal waters during a mild autumn/winter period in the Gulf of Lion". In: *Continental Shelf Research* 207, p. 104192. DOI: 10.1016/j.csr.2020.104192.

Millot, Claude (Apr. 3, 1979). "Wind induced upwellings in the Gulf of Lions". In: *Oceanologica Acta* 2.3, pp. 261–274.

— (Sept. 1990). "The Gulf of Lions' hydrodynamics". In: *Continental Shelf Research* 10.9, pp. 885–894. ISSN: 02784343. DOI: 10.1016/0278-4343(90)90065-T.

Millot, Claude and Lucien Wald (May 7, 1980). "The effect of Mistral wind on the Ligurian current near Provence". In: *Oceanologica Acta* 3.4, pp. 399–402.

— (1981). "Infra-red Remote Sensing in the Gulf of Lions". In: *Oceanography from Space*. Ed. by J. F. R. Gower. Boston, MA: Springer US, pp. 183–187. DOI: 10.1007/978-1-4613-3315-9_22.

Müller, Malte et al. (Mar. 2017). "AROME-MetCoOp: A Nordic Convective-Scale Operational Weather Prediction Model". In: *Weather and Forecasting* 32.2, pp. 609–627. DOI: 10.1175/waf-d-16-0099.1.

O'Neill, Larry W., Dudley B. Chelton, and Steven K. Esbensen (Sept. 1, 2012). "Covariability of Surface Wind and Stress Responses to Sea Surface Temperature Fronts". In: *Journal of Climate* 25.17, pp. 5916–5942. ISSN: 0894-8755, 1520-0442. DOI: 10.1175/JCLI-D-11-00230.1.

Obermann-Hellhund, Anika, Dario Conte, Samuel Somot, Csaba Zsolt Torma, and Bodo Ahrens (Jan. 2018). "Mistral and Tramontane wind systems in climate simulations from 1950 to 2100". In: *Climate Dynamics* 50.1, pp. 693–703. ISSN: 0930-7575, 1432-0894. DOI: 10.1007/s00382-017-3635-8.

Oke, Peter R. and Jason H. Middleton (Mar. 2000). "Topographically Induced Upwelling off Eastern Australia". In: *Journal of Physical Oceanography* 30.3, pp. 512–531. DOI: 10.1175/1520-0485(2000)030<0512:tiuoea>2.0.co;2.

Pairaud, I.L., J. Gatti, Nathaniel Bensoussan, R. Verney, and P. Garreau (Oct. 2011). "Hydrology and circulation in a coastal area off Marseille: Validation of a nested 3D model with observations". In: *Journal of Marine Systems* 88.1, pp. 20–33. ISSN: 09247963. DOI: 10.1016/j.jmarsys.2011.02.010.

Palma, Elbio D. and Ricardo P. Matano (June 2009). "Disentangling the upwelling mechanisms of the South Brazil Bight". In: *Continental Shelf Research* 29.11, pp. 1525–1534. ISSN: 02784343. DOI: 10.1016/j.csr.2009.04.002.

Pinazo, Christel et al. (2018). *Actions vers une Modélisation Intégrée Côtière Opérationnelle (AMICO). Phase 2. Projet collaboratif en Océanographie Côtière mis en place dans le cadre du " Programme GMES du Ministère du Développement Durable (GMES-MDD) "*. Research Report. Ministere du Developpement Durable, link : https://hal.archives-ouvertes.fr/hal-03624739/file/RapportAMICO_Phase2.pdf.

Powers, Jordan G. et al. (Aug. 2017). "The Weather Research and Forecasting Model: Overview, System Efforts, and Future Directions". In: *Bulletin of the American Meteorological Society* 98.8, pp. 1717–1737. DOI: 10.1175/bams-d-15-00308.1.

Puig, P, A Palanques, and J Guillén (Aug. 2001). "Near-bottom suspended sediment variability caused by storms and near-inertial internal waves on the Ebro mid continental shelf (NW Mediterranean)". In: *Marine Geology* 178.1, pp. 81–93. ISSN: 00253227. DOI: 10.1016/S0025-3227(01)00186-4.

Rey, Vincent, Jean-Luc Fuda, Didier Mallarino, Tathy Missamou, Caroline Paugam, Gilles Rougier, Isabelle Taupier-Letage, and Christiane Dufresne (May 2020). "On the use of long-term observation of water level and temperature along the shore for a better understanding of the dynamics: example of Toulon area, France". In: *Ocean Dynamics* 70, pp. 1–21. DOI: 10.1007/s10236-020-01363-7.

Reyes-Mendoza, Oscar, Ismael Mariño-Tapia, Jorge Herrera-Silveira, Gabriel Ruiz-Martínez, Cecilia Enriquez, and John L. Largier (May 2016). "The Effects of Wind on Upwelling off Cabo Catoche". In: *Journal of Coastal Research* 319, pp. 638–650. ISSN: 0749-0208, 1551-5036. DOI: 10.2112/JCOASTRES-D-15-00043.1.

Ross, Oliver N., Marion Fraysse, Christel Pinazo, and Ivane Pairaud (Mar. 2016). "Impact of an intrusion by the Northern Current on the biogeochemistry in the eastern Gulf of Lion, NW Mediterranean". In: *Estu-*

arine, Coastal and Shelf Science 170, pp. 1–9. ISSN: 02727714. DOI: 10.1016/j.ecss.2015.12.022.

Rossi, V., M. Feng, C. Pattiaratchi, M. Roughan, and A. M. Waite (July 2013). "On the factors influencing the development of sporadic upwelling in the Leeuwin Current system". In: *Journal of Geophysical Research: Oceans* 118.7, pp. 3608–3621. DOI: 10.1002/jgrc.20242.

Rossi, V., C. López, E. Hernández-Garcıa, J. Sudre, V. Garçon, and Y. Morel (Aug. 2009). "Surface mixing and biological activity in the four Eastern Boundary Upwelling Systems". In: *Nonlinear Processes in Geophysics* 16.4, pp. 557–568. DOI: 10.5194/npg-16-557-2009.

Rossi, V., A. Schaeffer, J. Wood, G. Galibert, B. Morris, J. Sudre, M. Roughan, and A. M. Waite (Jan. 2014). "Seasonality of sporadic physical processes driving temperature and nutrient high-frequency variability in the coastal ocean off southeast Australia". In: *Journal of Geophysical Research: Oceans* 119.1, pp. 445–460. DOI: 10.1002/2013jc009284.

Schaeffer, A., P. Garreau, Anne Molcard, Philippe Fraunie, and Yann Seity (June 2011). "Influence of high-resolution wind forcing on hydrodynamic modeling of the Gulf of Lions". In: *Ocean Dynamics* 61.11, pp. 1823–1844. DOI: 10.1007/s10236-011-0442-3.

Small, R.J., S. Carniel, T. Campbell, J. Teixeira, and R. Allard (May 2012). "The response of the Ligurian and Tyrrhenian Seas to a summer Mistral event: A coupled atmosphere–ocean approach". In: *Ocean Modelling* 48, pp. 30–44. DOI: 10.1016/j.ocemod.2012.02.003.

Stewart, Robert H. (2008). *Introduction to physical oceanography*. International Geophysics, url : https://hdl.handle.net/1969.1/160216.

Taupier-Letage, I. (2008). "On the Use of Thermal Images for Circulation Studies: Applications to the Eastern Mediterranean Basin". In: *Remote Sensing of the European Seas*. Ed. by Vittorio Barale and Martin Gade. Dordrecht: Springer Netherlands, pp. 153–164. DOI: 10.1007/978-1-4020-6772-3_12.

— (2014). *Thermosalinometer TRANSMED, Marfret Niolon, definitive data set*. In collab. with Isabelle.Taupier-Letage@Univ-Amu.Fr and SEDOO-OMP. Medium: ASCII type: dataset. DOI: 10.6096/MISTRALS-HYMEX.1127.

Taupier-Letage, I., I. Puillat, Claude Millot, and P. Raimbault (2003). "Biological response to mesoscale eddies in the Algerian Basin". In: *Journal of Geophysical Research: Oceans* 108.C8. DOI: https://doi.org/10.1029/1999JC000117. eprint: https://agupubs.onlinelibrary.wiley.com/doi/pdf/10.1029/1999JC000117.

Vannucchi, Valentina, Stefano Taddei, Valerio Capecchi, Michele Bendoni, and Carlo Brandini (Feb. 2021). "Dynamical Downscaling of ERA5 Data on the North-Western Mediterranean Sea: From Atmosphere to High-Resolution Coastal Wave Climate". In: *Journal of Marine Science and Engineering* 9.2, p. 208. DOI: 10.3390/jmse9020208.

Wessel, Pål and Walter H. F. Smith (Apr. 1996). "A global, self-consistent, hierarchical, high-resolution shoreline database". In: *Journal of Geophysical Research: Solid Earth* 101.B4, pp. 8741–8743. DOI: 10.1029/96jb00104.

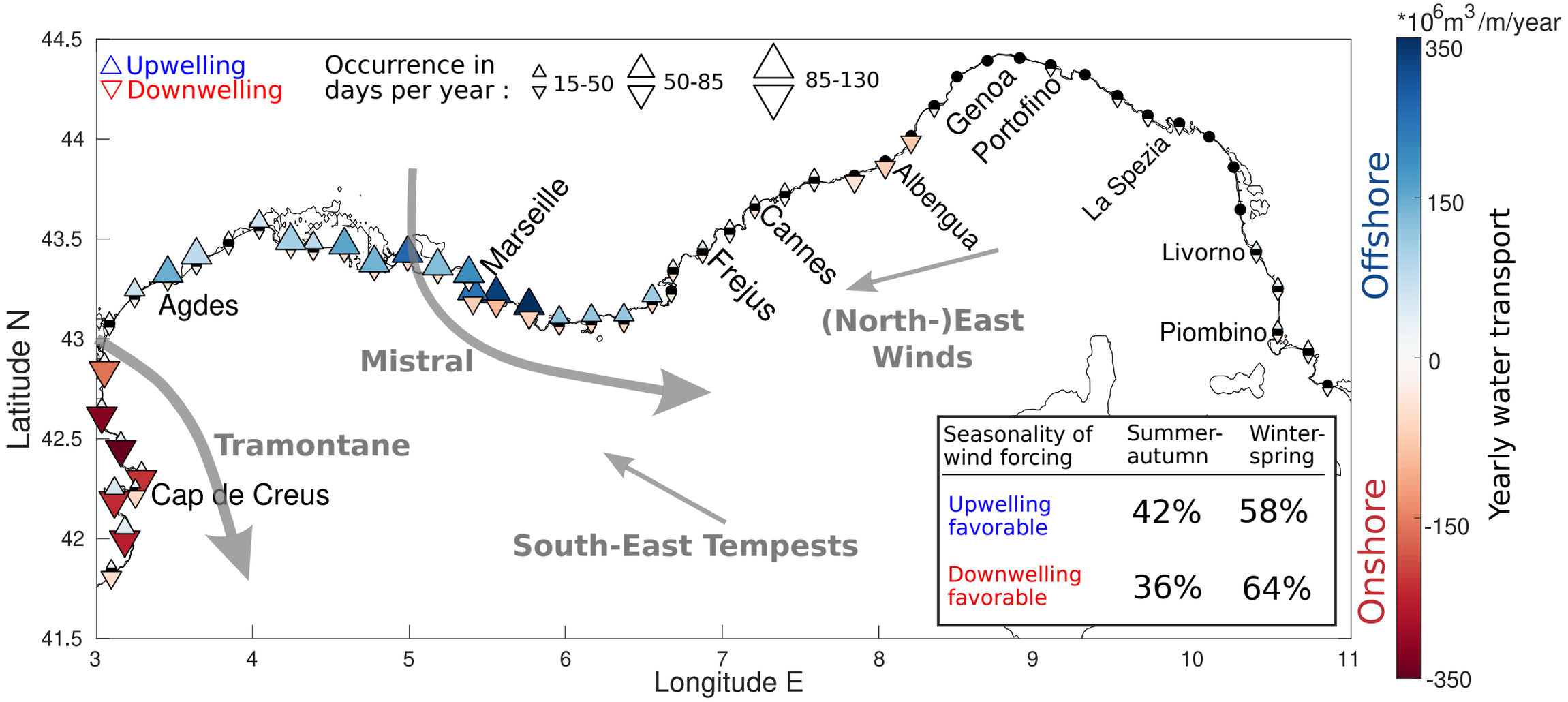
△Upwelling
▽Downwelling
Occurrence in days per year :
15-50
50-85
85-130
Agdes
Marseille
Frejus
Cannes
Albengua
Genoa
Portofino
La Spezia
Livorno
Piombino
Cap de Creus
Mistral
Tramontane
(North-)East Winds
South-East Tempests
Seasonality of wind forcing
Summer-autumn
Winter-spring
Upwelling favorable
42%
58%
Downwelling favorable
36%
64%
Latitude N
Longitude E
*10^6m^3/m/year
Offshore
Onshore
Yearly water transport